Effect of the addition of graphite nanoplatelets on the efficiency of Bi_2Te_3-based thermoelectric materials by powder metallurgy.

Submitted by:
Manuela Castañeda Montoya

Research work submitted as a partial requirement for the degree of:
Master in mechanical engineering

Advisor:
Prof. Henry Alonso Colorado Lopera, PhD

Co-advisor:
Prof. Claudio Aguilar, PhD

Line of research:
Composite Materials
Research Group:
Cements, Ceramics and Composites (CCComposites)

Universidad de Antioquia
Faculty of Engineering, Mechanical Engineering Department
Medellín, Colombia
2023

Cita	Castañeda Montoya [1]
Referencia Estilo IEEE (2020)	[1] M. Castañeda Montoya, "Effect of the addition of graphite nanoplatelets on the efficiency of Bi2Te3-based thermoelectric materials by powder metallurgy". Tesis de maestría, Maestría en Ingeniería Mecánica, Universidad de Antioquia, Medellín, Antioquia, Colombia, 2022.

Maestría en Ingeniería Mecánica, Cohorte VII.

Grupo de Investigación Cements, Ceramics and Composites (CCComposites).

Centro de Investigación Ambientales y de Ingeniería (CIA).

A Dios por dame fuerza en los momentos difíciles. A mis padres Blanca Nubia Montoya y Jesús Antonio Castañeda y a mi hermano Santiago por siempre ayudarme, apoyarme y darme motivación.

ACKNOWLEDGEMENTS

To Colombia Científica who, through the "Alliance for the energy sustainability of the Colombian industrial and transport sectors through the use of regional renewable resources", SÉNECA, financed the internship for my academic and research training within the framework of the project (P10) entitled: Ajuste, escalado y evaluación en condiciones de procesos productivos industriales de sistemas de combustión avanzados de alta eficiencia energética y bajas emisiones.

PhD. Henry Alonso Colorado Lopera and PhD. Claudio Aguilar, my advisors of this degree work, for his continuous support and for making the development of this research possible.

To the center for research, innovation, and development of materials CIDEMAT and the research group Gimacyr, for facilitating my entry to their laboratories and lending me their equipment for the development of my master's thesis.

To my parents and brother, for always supporting me and giving me the strength to continue in difficult times.

ABSTRACT

In this research, a comprehensive systematic search was conducted to present an overview, including trends and limitations, in research related to thermoelectric materials. As a result of this analysis, it was found that the aspects related to costs and initiatives associated with circular economy models have been little explored, which represents not only an opportunity for the development of new approaches in the conception of thermoelectric systems, but also for the conception of optimized designs that address the current limitations of this technology. The main objective of this work is to develop a thermoelectric material composed of P-type BiTe base and different percentages by weight of graphite nanoplatelets (0, 0.1%, 0.5 and 1%wt of GNP). This development is complemented by the physicochemical characterization of the raw materials, the ground powders and the formed material, the characterization techniques used were scanning electron microscopy and X-ray diffraction and its thermoelectric properties such as electrical conductivity (S / m), mobility (cm2 ((Vs)), Hall coefficient (cm3 / ° C) and Seebeck coefficient (μV / K). Although the addition of graphite nanoplate did not present a noticeable improvement in the properties thermoelectric, the fabricated materials did present improvements in the properties with respect to thermoelectric evaluated in comparison to those published in the literature. Finally, the characterization of low-cost BiTe base thermoelectric modules typically used for generation (SP1848-27145SA (TEG-GEN)) and cooling (TEC1-12706 (TEC-REF)), both used in this research for heat recovery, was performed. The modules were evaluated against various configurations, distances from the heat source and distributions, to determine the optimal recovery conditions. The experiments were conducted at the laboratory level and in a large-scale kiln of the traditional ceramic industry and revealed that even cooling modules are suitable for energy recovery, particularly in developing countries, where other generators are more expensive and difficult to obtain. These thermoelectric generators were tested for low-temperature heat recovery in regular furnaces to be deployed elsewhere. The results show that even thermoelectric cooling modules can be a solution for heat recovery in many heat sources, particularly strategic for developing countries.

Key words: Thermoelectric materials, thermoelectric modules, composite materials, characterization, type p-BiTe, graphite nanoplatelets

RESUMEN

En esta investigación se realizó una búsqueda sistemática exhaustiva para presentar una visión general, incluyendo tendencias y limitaciones, en la investigación relacionada con los materiales termoeléctricos. Como resultado de este análisis, se encontró que los aspectos relacionados con los costos y las iniciativas asociadas a los modelos de economía circular han sido poco explorados, lo que representa no solo una oportunidad para el desarrollo de nuevos enfoques en la concepción de sistemas termoeléctricos, sino también para la concepción de diseños optimizados que aborden las limitaciones actuales de esta tecnología. El objetivo principal de este trabajo es desarrollar un material termoeléctrico compuesto de base P-type BiTe y diferentes porcentajes en peso de nanoplaquetas de grafito (0, 0.1%, 0.5 y 1%wt de GNP). Este desarrollo se complementa con la caracterización fisicoquímica de las materias primas, los polvos molidos y el material conformado, las técnicas de caracterización utilizadas fueron microscopía electrónica de barrido y difracción de rayos X y sus propiedades termoeléctricas como la conductividad eléctrica (S/ m), movilidad (cm^2((Vs)), coeficiente Hall (cm^3/°C) y coeficiente Seebeck (µV/K) aunque la adicción de las nanoplaquetas de grafito no presentaron una mejora notoria en las propiedades termoeléctricas, los materiales fabricados si presentaban mejoras en las propiedades con respecto termoeléctricas evaluadas en comparación a los publicados en la literatura. Finalmente, se realizó la caracterizaron de módulos termoeléctricos base BiTe de bajo costo típicamente utilizados para generación (SP1848-27145SA (TEG-GEN)) y refrigeración (TEC1-12706 (TEC-REF)), ambos utilizados en esta investigación para la recuperación de calor. Los módulos se evaluaron contra varias configuraciones, distancias con respecto a la fuente de calor y distribuciones, con el fin de determinar las condiciones óptimas de recuperación. Los experimentos se realizaron a nivel de laboratorio y en un horno a gran escala de la industria cerámica tradicional, y revelaron que incluso los módulos de refrigeración son adecuados para la recuperación de energía, particularmente en los países en desarrollo, donde otros generadores son más caros y difíciles de obtener. Estos generadores termoeléctricos se probaron para la recuperación de calor a baja temperatura en hornos regulares para ser implementados en otros lugares. Los resultados muestran que incluso los módulos de refrigeración termoeléctrica pueden ser una solución para la recuperación de calor en muchas fuentes de calor, particularmente estratégicas para los países en desarrollo.

Palabras clave: Materiales termoeléctricos, módulos termoeléctricos, materiales compuestos, caracterización, BiTe tipo p, nanoplaquetas de grafito.

Table of Contents

List of Figures

List of Tables

CHAPTER 1

1. Introduction

1.1. Problem Statement

At present the search for new ways to generate clean energy has become one of the priorities of engineering work, in different studies it has been reported that about 60% of the energy produced worldwide ends up as waste heat in different sectors such as transport, industry and construction [1]–[6]. The use of this waste heat represents energy savings and a reduction in greenhouse gas emissions expelled into the environment[4]. Thermoelectric materials represent great interest because they are an alternative to take advantage of ecological energy through the recovery of waste heat generated during different processes and the recovered heat can be used as electrical energy to feed the same process making it more efficient[3], [7], [8].

Despite the different advantages of this type of materials, they also have great limitations such as their low efficiency or performance, which currently hardly exceeds 10%.[9]. This is because these materials must be good at transmitting electricity, but not heat, to ensure that the temperature between their ends is different. Raw materials and manufacturing methods also represent great challenges, because most of them are expensive, scarce and are decisive for obtaining a material with good properties.[10]–[13].

Bismuth tellurium (Bi_2Te_3) is one of the most commercial thermoelectric materials at the time, due to its low cost and easy manufacture. This material is considered a low temperature thermoelectric because its applicability only reaches up to 300 ° C. However, this material does not have a good efficiency, so different physical and chemical methods have been investigated to increase its efficiency. The use of dopants to raise electrical conductivity and manufacturing by different methods such as supergrids, nano materials to decrease thermal conductivity are some ways developed to improve the efficiency of this material[14]–[18]

In this aspect, carbon-based materials and nanomaterials have been widely studied since they have excellent electrical and thermal properties, so they are the focus of many investigations in which it has been observed that the addition of graphene, graphite and their oxides, carbon nanotubes, etc., has managed to reduce the thermal conductivity of the material because in some cases these work as a barrier in the transport of phonons and at the same time allow to maintain or increase the electrical conductivity in the material[19]–[24]

So far, graphite nanoplatelets have been studied to improve properties in mechanical, thermal, electrical, electrochemical, anticorrosive materials in polymeric, construction and metallic materials.[25]–[28]

Considering the above, the following question arises: Could improvements in thermoelectric and physicochemical properties be obtained by incorporating different percentages of graphite nanoplatelets in a matrix of Bi_2Te_3 through a process of grinding balls under controlled atmosphere, to then be cold pressed and sintered in a furnace with controlled atmosphere?

1.2. Objectives

1.2.1. General objective

- To evaluate the effect of the addition of graphite nanoplatelets by powder metallurgy on the efficiency of the Bi2Te3 alloy.

1.2.2. Specific objectives

- Characterize graphite nanoplatelet base materials and Bi2Te3.
- Determine parameters of the manufacturing process by the method of powder metallurgy in controlled atmosphere and characterization of the material graphite nanoplatelets- Bi2Te3.
- Evaluate Bi2Te3-based commercial cells in power generation applications.

CHAPTER 2

2. Theoretical Framework and State of Art

2.1. Theoretical Framework: Sustainability and circular economy perspectives of materials for thermoelectric modules: a systematic review. Published in Sustainability magazine in May 2022. DOI: 10.3390/su14105987 [29]

2.1.1. Methodology systematic search

In order to find the topic for this review, a systematic search was initially made in the Scopus database using the keywords "thermoelectric AND modules" with the AND logical connector. In this initial search a total of 4676 results were obtained. Then, 2 filters were used to refine the search. In a first filter, only selected revision type documents were selected; while in a second filter, the publication date was restricted from 2015 to 2020, finally obtaining a total of 61 reviews, as shown in **Table 1**.

Table 1. Summary of the initial systematic search for the subject of the review.

Database	Number of articles found		
	Unfiltered	Filter 1	Filter 2
Scopus	4676	81	61

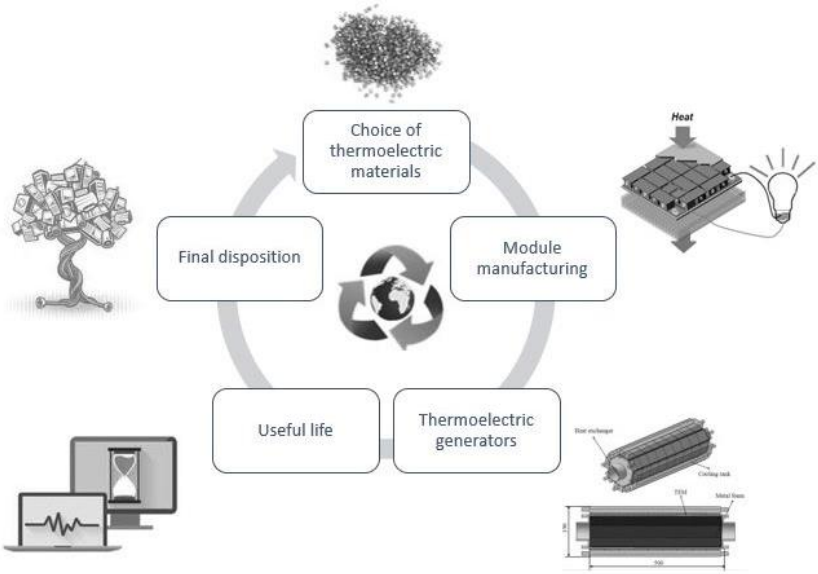

Figure 1. Themes of the article towards the circular economy of thermoelectric modules.

Figure 2 presents the classification of the works judged in the initial bibliographic review according to their content, in four categories: TE materials, TEG modules, applications and sustainability, which were chosen by grouping different themes and subtopics. This was done by reading the titles, abstract and keywords. From this selection, it was found that 10 articles were not relevant to the topic of TE materials, and, out of the 51 relevant articles, some were classified in two of the categories.

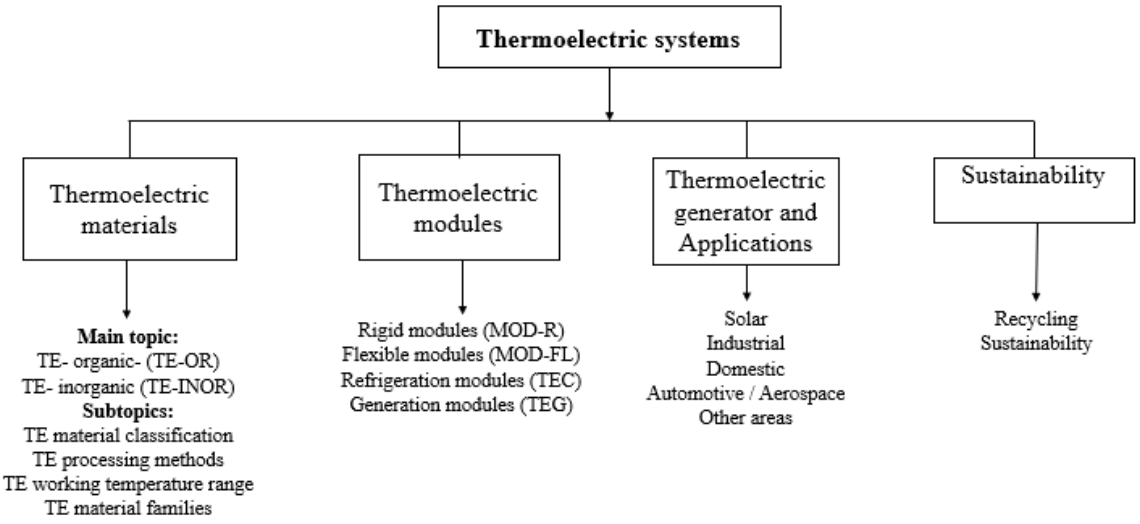

Figure 2. Topics found in the articles of the initial systematic search.

In this initial systematic search, a knowledge gap was found in the sustainability category in which themes of profitability, cost / efficiency ratio, recycling, among others, were developed. For this reason, it was decided to take this approach to carry out the present analysis.

Regarding the development of this review, 6 base themes that lead to the sustainability of this type of materials were considered: efficiency, cost, recycling, sustainability, life cycle and profitability. For this, after the deduplication of the articles, 4 filters were applied. The first filter was the year of publication in which only the articles published from 2010 to 2020 were considered. The second filter was the type of document, in this case only the research articles were considered. The third filter was based on reading the title and abstract. And finally, a thorough reading of the purified articles was carried out, which resulted in a total of 36 relevant articles, from which the analysis presented below was developed. Table 2 shows the search strings used and the result of their systematic debugging. Likewise, Figure 3 shows the results of the search carried out, where Figure 3(a) shows the data obtained in percentage for each search string. Figure 3(b) shows a classification of the publications analyzed by year, revealing the growing interest in TEG. In Table 3, the publications and topics covered by each of these strings are presented according to the topics to be addressed in this study.

Table 2. Search strings and filters used in systematic search.

Search strings	**Number of articles found**				
	Unfiltered	**Filter 1**	**Filter 2**	**Filter 3**	**Filter 4**
"Thermoelectric" AND "Modules" AND "Recycling"	37	23	22	6	5

"Thermoelectric" AND " Modules" AND "Cost" AND "Efficiency"	211	115	105	25	12
"Thermoelectric generators" AND "Cost" AND "Efficiency"	298	249	143	9	5
"Thermoelectric generators" AND "Sustainability"	25	24	13	5	4
"Thermoelectric" AND "Modules" AND "Life cycle"	25	19	11	3	2
"Thermoelectric modules" AND "demand"	43	38	24	5	1
"Thermoelectric" AND "Materials" AND "Modules" AND "Cost" AND "efficiency"	92	77	45	22	7
Filter 1: Year of publication of the article from 2010 to 2020, Filter 2: type of document "article type", Filter 3: reading of title and summary, Filter 4: reading the article.					

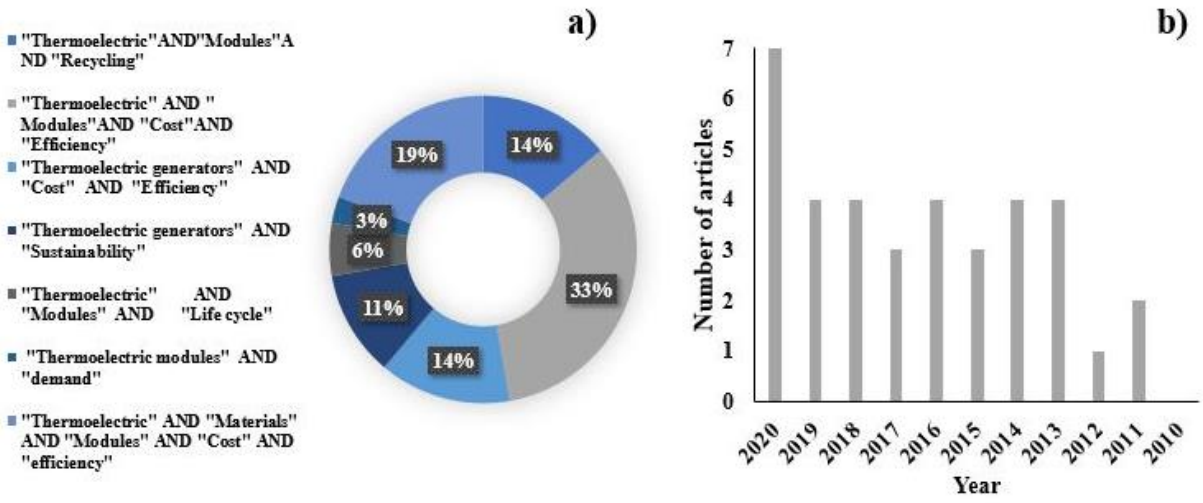

Figure 3. Systematic search results for (a) number of articles found per chain, and (b) number of articles per year.

Table 3. Articles found in the systematic search with their classification by subject matter.

Ref.	Year	MAT	MOD	TEG	COST	EFF	MDL	RE
[30]	2020	X	X			X		
[31]	2020		X			X	X	
[32]	2020		X		X	X		
[33]	2020		X	X	X	X	X	

[34]	2020			X	X	X	X	
[35]	2020		X	X		X		
[36]	2020		X					X
[37]	2019	X				X	X	
[38]	2019		X		X	X	X	
[39]	2019		X			X	X	
[40]	2019		X					
[41]	2018	X			X	X		
[42]	2018		X			X	X	
[43]	2018		X			X	X	
[44]	2018	X	X		X	X	X	
[45]	2017		X					X
[46]	2017		X					X
[47]	2017	X	X			X		
[48]	2016	X	X		X	X	X	
[49]	2016		X			X	X	
[50]	2016			X	X		X	
[51]	2016			X	X	X	X	
[52]	2015	X	X			X		
[53]	2015		X	X		X	X	
[54]	2015	X	X			X	X	
[55]	2014		X	X		X	X	
[56]	2014		X			X		
[57]	2014		X				X	
[58]	2014		X					X
[59]	2013		X		X	X		
[60]	2013	X	X	X		X		
[61]	2013		X					X
[62]	2013			X	X	X	X	
[63]	2012		X		X		X	
[64]	2011	X	X			X		
[65]	2011					X		

MAT: TE materials, MOD: Thermoelectric modules, TEG: Thermoelectric generators, EFF: Efficiency, MDL: Modeling and RE: Recycling.

2.1.2. Thermoelectric materials

It is estimated that between 50% and 80% of the studies related to thermoelectric generation systems (TEG) correspond to the TE materials themselves. Therefore, the development of materials that have

a low cost and high efficiency is one of the most important pillars to achieve the commercial profitability of this type of systems.[36], [66]

In the systematic search carried out, 10 articles were found in which the TE material was studied in depth in order to increase its efficiency, decrease costs or develop viable materials in both environmental and sustainability aspects by analyzing factors such as its abundance and its degree of toxicity among others. Table 4 presents a classification of these items according to the cost, efficiency and sustainability of the TEG modules. In this table, the cost column expresses the materials cost reduction with a minus sign (-), and the materials cost increase with a plus sign (+). In this aspect the elements that compose in some cases the type of processing is taken into account. Please note that in most of the articles reviewed, the cost of the material was not stated explicitly. For efficiency, the minus sign refers to materials with low efficiencies (ZT <1) and the plus sign (+) for materials with significant efficiencies (ZT> 1). Finally, the sustainability of the materials is valued from environmental aspects such as the availability, toxicity and useful life, therefore the minus sign indicates that it is unsustainable and the plus sign that it is sustainable.

Table 4. Classification of the articles found according to the results obtained in the development of thermoelectric materials.

Ref	Cost	Efficiency	Sustainability	Year
[30]	-	+	-	2020
[37]	-	-	+	2019
[41]	-	+	-	2018
[44]	+	+	+	2018
[47]	-	-	+	2017
[48]	-	+	+	2016
[52]	-	+	-	2015
[54]	-	-	+	2015
[60]	-	+	+	2013
[64]	-	+	+	2011
Cost: -Low cost, +high cost **Efficiency: + high efficiency and – low efficiency** **Environmental aspects and sustainability: - unsustainable and + more sustainable**				

From the articles related in Table 3, three case studies were found [5], [67], [68] that ex- amined cost of TE materials, including their cost effectiveness and the processing technique used to develop them. Among the cost-effective materials, the use of oxides as raw materials stands out. Hung et al.[54] studied different oxides (Na_2CoO_4, $Ca_3Co_4O_9$, ZnO, $SrTiO_3$ and $CaMnO_3$) in order to decrease costs in the manufacture of TEG modules since the cost of manufacturing the oxides is approximately US $ 1.1 /kg, which is equivalent to only a quarter of composite materials composed of metals and rare earths. On the other hand, Lee et al.[47] studied the potential of TiO2-x

for TE materials manufactured by plasma deposition. Ozturk et al. [37] studied two types of oxides: $Ca_{2.5}Ag_{0.3}X_{0.2}Co_4O_9$ type n and $Zn_{0.96}Al_{0.02}Y_{0.02}O$ type n, where X and Y are different dopants manufactured using the sol-gel method. In these works, the benefits of using oxides as raw materials are highlighted. Among these benefits are low cost, abundance, resistance to high temperatures, as well as simplified manufacturing processes not requiring controlled atmospheres. However, it can be seen that the purpose of these studies is to improve the efficiency of materials. In Table 5 it can be seen that the oxides present the least merit (efficiency). According to the review, the modules' oxide-based TEGs can increase their efficiency through the use of special processing [45] or doping techniques [31], which makes their use more viable.

Table 5. Thermoelectric materials type, merit rating, and temperature.

Material	Type	ZT	T (°C)	Ref.	Material	Type	ZT	T (°C)	Ref.
SnSe	p	2.5	627	[44]	$Pb_{0.93}Sb_{0.05}S_{0.5}Se_{0.5}$	n	1.7	627	[69]
FeNbSb	p	1.5	927	[52]	$Si_{80}Ge_{20}$	n	1.5	727	[44]
Bi_2Te_3	p	0.9	100	[43]	AgPbmSbTe$_2$+m	n	2	527	[44]
Na_2CoO_4	p	0.75	527	[54]	$Cu_xBi_2Te_{2.7}Se_{0.3}$	n	1	127	[44]
$Ca_{2.5}Ag_{0.3}Eu_{0.2}Co_4O_9$	p	0.57	800	[37]	$Mg_2(Si_{0.4}Sn_{0.6})_{0.99}Sb_{0.01}$	n	0.8	327	[35]
$Ca_{2.5}Ag_{0.3}Er_{0.2}Co_4O_9$	p	0.54	800	[37]	$Mg_2(Si_{0.53}Sn_{0.4}Ge_{0.05}Bi_{0.02})$	n	1.4	527	[35]
$Ca_{2.5}Ag_{0.3}Nb_{0.2}Co_4O_9$	p	0.52	800	[37]	ZnO	n	0.6	902	[54]
$Ca_{2.5}Ag_{0.3}Sm_{0.2}Co_4O_9$	p	0.51	800	[37]	$SrTiO_3$	n	0.4	827	[54]
$Ca_{2.5}Ag_{0.3}Lu_{0.2}Co_4O_9$	p	0.50	800	[37]	$CaMnO_3$	n	0.3	902	[54]
$Ca_3Co_4O_9$	p	0.5	827	[54]	$Zn_{0.96}Al_{0.02}Ge_{0.02}O$	n	0.04	800	[37]
$Mm_{0.28}Fe_{1.52}Co_{2.48}Sb_{1.2}$	p	0.5	477	[49]	$Zn_{0.96}Al_{0.02}Ga_{0.02}O$	n	0.17	800	[37]
Ca2.5Ag0.3Yb0.2Co4O9	p	0.47	800	[37]	$Zn_{0.96}Al_{0.02}In_{0.02}O$	n	0.12	800	[37]
$MnSi_{1.75}Ge_{0.01}$	p	0.4	527	[35]	$Mg_2Si_{0.4}Sn_{0.6}$	n	1.2	450	[43]
$MnSi_{1.81}$	p	0.3	400	[43]	Bi_2Te_3	n	0.8	100	[43]
$Ca_3Co_2O_6$	p	0.25	877	[43]	TiO_{2-x}	n	0.132	477	[31]]
H-SnSe	p	2	427	[44]	Ni	n	0.020	477	[31]
BiBaCuSeO	p	1	527	[43]	$Yb_{0.09}Ba_{0.09}La_{0.05}Co_4Sb_{12}$	n	1.2	477	[49]
PbTe-SrTe+Te 2%	p	1	350	[41]	$Pb_{0.93}Sb_{0.05}S_{0.5}Se_{0.5}$	n	1.7	627	[30]

On the other hand, the use of cheap and abundant materials such as lead-based materials or silicides has also been the subject of recent studies. Han et al. [41] studied the feasibility of PbTe-SrTe base materials doped with 2% Te. They concluded there was a cost reduction through a low-cost processing method such as stable screen printing, although one of the base materials and the tellurium are high cost and low abundance elements. Jiang et al. [30] proposed PbS as an alternative to the base material PbTe, arguing that by doping with Sb and Se, efficiency can be considerably improved, in addition to them being abundant and low-cost materials.

Fu et al.[52] and Salvador et al.[60] developed materials such as FeNbSb (Half- Heuslers) and $Yb_{0.09}Ba_{0.09}La_{0.05}Co_4Sb_{12}$ (skutterudite), respectively, which are composed of low-cost and abundant elements, and by doping techniques are able to increase their efficiency. However, Ouyang et al. [44] evaluated some of the latest generation materials and recommended that materials such as skutterudites and half-heuslers could only be used in applications where cost is not of concern, due to the high manufacturing costs of these materials. On the other hand, Skomedal et al. [48] suggested the use of magnesium silicides as a favorable TE material, due to their low cost, abundance and low toxicity, despite their low efficiency when doping with elements such as Sn and Sb. They concluded that materials based on magnesium silicides are recommended for applications where low cost or low weight are more important than efficiency.

In addition, Homm et al. [64] analyzed some TE materials such as SiGe, PbTe, Bi2Te3, FeSi2 and ZnO. The authors classified them according to selection criteria for different applications that required certain specifications for temperature, efficiency, and cost, but taking into account the environmental aspects that each one presented.

According to the present review, it is observed that there is a conflict between the aspects of cost, efficiency, and sustainability. Figure 4 presents a classification based on these aspects of recent studies addressed in this analysis. Three articles were found involving costs and efficiency in zone A, [30], [35], [52] three articles between costs and sustainability in zone B [37], [47], [54]; one article involving efficiency and sustainability in zone C [44]; and tree articles involving all aspects, costs, efficiency and sustainability in zone U [48], [60], [64]. From this classification it is concluded that the oxides are inexpensive TE materials with important advantages. In particular, they are abundant, do not require high-cost processing, and resist high temperatures, which prevents premature degradation of the TE material. Moreover, they enable the formation of robust materials with a longer useful life and have a good cost-sustainability ratio. However, their efficiency is reduced with respect to the commercially used TE materials, which prompts us to think about the different research approaches to improve them, such as nano-structuring, electronic band engineering, quan- tum confinement, as well as strategies such as crystal electron glass phonon, doping, and introduction of defects, among others. However, the use of any of these techniques requires specialized and complex processes, which would be reflected in the final cost of the product and would probably mean that the cost-efficiency ratio is not viable for developments in a commercial environment. Therefore, the development of this research is of utmost importance for providing not only a better future perspective of TE materials, but also because there are few investigations that specifically address the economic component of these materials.

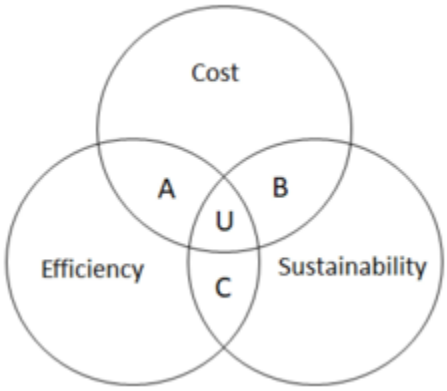

Figure 4. Classification of the articles found according to the results obtained for TE materials.

Furthermore, from a sustainability perspective, little information is available on commonly used TE materials. An example of this is the use of toxic materials such as lead, tellurium and bismuth in their fabrication. Therefore, an important aim of research is to explore is the environmental risks that these materials can present at different stages of the useful life of TEG modules and to search for abundant and low-cost elements.

Interest in certain thermoelectric materials is based on a combination of their characteristics and performance. Figure 5 shows the trends in the number of publications in recent years in relation to some representative thermoelectric materials, according to a survey carried out in the Scopus database. The figure shows the growing research interest in these thermoelectric materials.

Recent Development of New Materials for Thermoelectric Applications

The increases in the ZT values are produced especially by the decrease in the thermal conductivity of crystal lattices, and the recent advances in the development of new TE materials are based on the search for mechanisms that make it possible to minimize the thermal conductivity in the crystal structures of TE materials. Advances in TE materials provide measurable improvements in ZT values through the use of nanotechnology-based techniques. Nanophonon metamaterials provide special local resonance states in semiconductor materials for suppression of thermal conductivity. According to Ouyang et al. [70], nascent theories are being forged in the field of TE materials. Among the most promising are the coherent phonon theories (https://www.nature.com/articles/nmat3826, aacessed on 23 August 2021), the nanophonon metamaterial [61], the rattling effect [62], the topological phonon [70], [71] and the topological electron [72]. Likewise, the synthesis of low-dimensional materials would allow the separation of related thermoelectric parameters to optimize thermoelectric performance. Among the advances in this field, the 1D Nanowires stand out [73], [74], as well as the 2D Materials [75], [76] and the Nanomesh Structures [77], [78] . Finally, it should be noted that given the recent advances in computing, artificial intelligence and machine learning in combination with atomic simulation techniques, the development of new tools to predict new structures and

characteristics of novel materials is envisioned, and these will provide accurate forecasts of the inherent properties of TE materials.

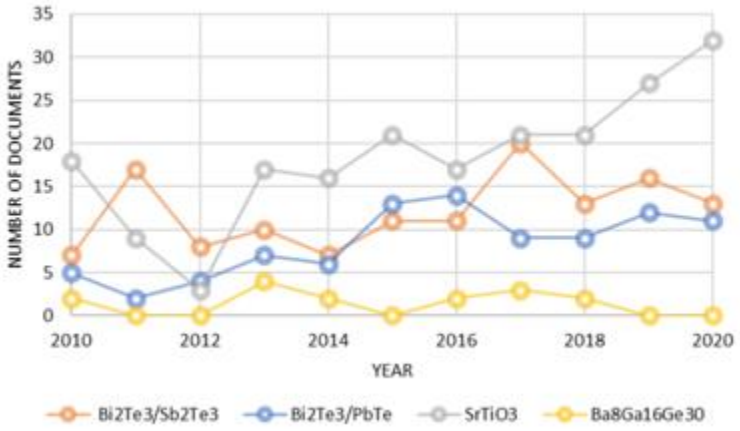

Figure 5. Research in thermoelectric materials in recent years.

2.1.3. TEG modules

In the systematic search carried out, 29 articles related to TEG modules were found. We observed that one of the most commonly addressed topics is the efficiency/cost relationship presented by TE materials. This aspect is usually approached from several points of view, such as cost reduction, varying the TE material, or through a design of the TEG module that preserves its efficiency. However, another important factor that must be taken into account is the sustainability of the modules, which ranges from the analysis of their useful service life to the study of their final disposal. In Figure 6, the classification of the articles according to their content can be observed. These were classified by costs, sustainability, efficiency and modeling. In this graph, one article as found classified involving costs [50]; seven involving efficiency [30], [47], [52], [57], [60], [64], [65]; one in modelling [56]; and six in sustainability [36], [40], [45], [46], [58], [61]. In the common areas D, E, F, G, H, it was not found papers between costs and sustainability and costs and modelling in zones D and G respectively. Between costs and efficiency, zone E, three articles were found [32], [36], [63]; while for zone F, between efficiency and modelling, seven were found [31], [42], [43], [50], [55], [79] Finally, ten references were found in thermoelectric modules, zone H [33], [34], [37]–[39], [44], [48], [49], [51], [63]

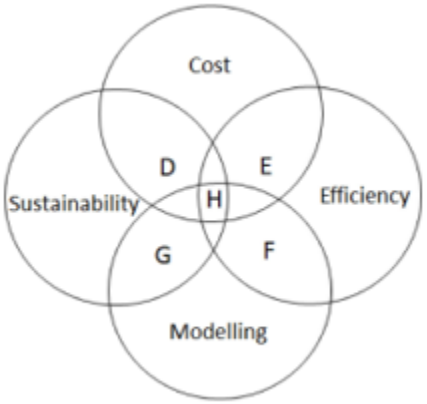

Figure 6. Classification of the articles found according to the results obtained for thermoelectric modules.

2.1.3.1. Cost / Efficiency

Currently, TEG modules do not present a high demand as would be expected as they are a clean source of energy that does not require exhaustive maintenance. However, the high cost / efficiency ratio that TEG modules present means that their introduction into the industry is difficult and with still limited their viability.

2.1.3.2. Module manufacturing

With the aim of decreasing the production costs without affecting the efficiency of the modules, some authors focus their research on the design of TE modules, the search for new materials in order to decrease costs or increasing their efficiency. The use of oxides, half-heusler materials, skutterudites, and composite materials (organic/inorganic) can be a solution to overcome the limitations of the TEG modules. It is important, however, that these studies be developed in a holistic context oriented to applicability.

Studies such as those by Salvador et al. [60] , on skutterudite encapsulated modules with a ZT of 1, enable this type of module to compete directly with the efficiencies of commercial PbTe modules. However, to date, commercial modules with this type of materials are scarce and costly due to their current manufacturing methods. Fu et al. [52] [valuated the potential of doped half-heusler materials with an efficiency of 6.2% and a power density of 2.2 W/cm^2. These modules can resist high temperatures (~927 ˚C) and are an economical alternative to commercially used TE materials.

In order to reduce costs in TEG modules and to improve their coupling to any surface, Lee et al. [47] studied the manufacture of TEG devices and basic electronics using titanium oxides (which operate at temperatures ~500 ˚C), and deposited them by plasma sintering, thus obtaining an assembly of thermocouples connected in series and in parallel with an efficiency of 0.85% and an

electrical power of 2.43 mW at 450 ˚C. The authors did not conduct an economic analysis on the assembly, only referring to its easy and low manufacturing cost through the elimination of many of the parts that make up the commercial TEG modules. On the other hand, Yazawa et al. [62] proposed the use of flexible modules that incorporate organic/inorganic composite materials and reduce costs but with a reduced performance (ZT between 0.01 and 0.25), a performance that is relatively low compared with commercial TE materials.

Anderson et al. [40] carried out a techno-economic analysis on the total cost of TEG devices, finding that the use of impure TE materials such as oxides or other types of cheaper TE materials are not the most feasible option at a cost level, since TE material only represents 15% of the total value of a TEG module.

Table 6 presents some characteristics of commercial modules such as base material, dimensions, power output, open circuit voltage, operating temperature range and cost. Currently, the most common TEG modules are those manufactured from bismuth telluride. Among these, a great variety can be found in which characteristics such as their configuration, output power and circuit voltage might vary. Most modules can work at maximum temperatures between 320 ˚C and 350 ˚C, but their optimal operating conditions are around 250 ˚C. These types of modules can be found in the market with prices ranging between
$10 and $28 US.

Likewise, commercially it is possible to find modules that resist higher temperature ranges, such as TEG PbTe-BiTe modules. These TEG modules can work at maximum temperatures of around 360 ˚C, and commercially they can be found with better output powers than the BiTe based ones. Naturally, the improvement of these characteristics is reflected in their cost.

Table 850 ˚C reaching 6% efficiency, being attractive for the recovery of residual heat at high temperatures. However, this type of component is up to seven times the cost of traditional BiTe-based modules. This makes them less attractive due to their cost-efficiency ratio.

Table 6. Technical characteristics and cost of commercial modules.

Commercial modules	Materials	Dimensions (W*L*H) (mm)	Output power (W)	Open circuit voltage (V)	Operating temperature range	Cost ($US)
Hz-1	BiTe based	29.21*29.21*5.08	2.3	6.1	250 to 50°	$10.00
Hz-9	BiTe based	62.74*62.74*6.63	9	6.1	250 to 50°	$15.00
Hz-14	BiTe based	62.74*62.74*6.63	14	3.1	250 to 50°	$25.00
Hz-14HV	BiTe based	61.05*71.05*7.87	14	8	250 to 50°	$25.00

Hz-20	BiTe based	74.68*74.68*5.08	20	4.5	250 to 50°	$50.00
Hz-20HV	BiTe based	74.50*68.00*5.00	20	10.8	250 to 50°	$50.00
TEP1-1264-3.4	BiTe based	40.5*40.5* __	5.4	10.8	300 to 30°	$40.89
TEG1-126610-5.1	BiTe based	40.5*40.5* __	5.1	7.8	300 to 30°	$28.41
TEM 070-6006	SnTe based	40*40*4	16.8	-	630 to 70	-
TEG1-PB-12611-60	PbTe-BiTe	56*56* _	21.7	9.2	350 to 30°	$69.00
CMO-32-62S	BiTe cold site-Calcium manganese oxide hot site	64.5*64.5*8.3	12.30	12.8	800 to 50°	$375.00
CMO-25-42S		42*42	7.5	10.0	800 to 50°	$330.00

2.1.3.3. Module design

Commercial modules, such as those from Table 6, generally have a pre-designed configuration from the supplier, which means that for some applications, they are not suitable or do not show their optimal performance. On the other hand, the design is an important factor since by means of the design parameters, the efficiency, the cost and the useful life of the modules can be improved. Likewise, most of the studies related to TEG components or systems are carried out using simulation tools [80] , due to the complexity of their manufacture, as well as the cost that these would generate for their development if they were carried out exclusively by experimental means. Some of the most relevant studies in this regard are listed below.

Segmented modules represent one of the most viable alternatives from the viewpoint of design. In these, various TE materials are used to manufacture the module legs, seeking to increase the working temperature, minimize the thermal effects, and increase the efficiency of the TEG modules. Recent work related to the manufacture of segmented modules includes the work of Hung et al. [54], who implemented commercial TE materials in cold areas of the cell and oxides in hot areas, in order to increase the working temperature of the modules. The viability of these TEG modules was analyzed using numerical modeling, which found that the oxide-segmented modules have an efficiency of around 10%. Ouyang et al. [44] carried out a study in which high-ZT TE materials were evaluated by finite element analysis. A systematic model was achieved for the segmented modules, finding a cost-performance ratio of $ USD ~0.86/W with an efficiency of 17.8%. Similarly, Jiang et al. [30] evaluated a TEG module composed of np Bi2Te3 and np PbS/PbTe, which exhibited an efficiency of

11.2% with a ΔT = 317 ◦C. In addition, they optimized the ratio of the legs at low and high temperatures, determining the optimal ratio to be 7:17. The maximum power obtained in this TEG module was 0.53 W for a ΔT = 312 ◦C.

During the design of TEG modules, the optimization of parameters such as the length of the legs or the number of thermocouples of the TE materials helps to reduce the amount of material used, without compromising the efficiency of the modules. According to Rezania et al. [57], the temperature differences at the n- and p-type junctions of TE elements are not identical. Such temperature differences are lower in n-type TE elements, compared with those in p-type TE elements, due to the higher thermal conductivity in the n-type material. Consequently, the footprint size of the n-type element must be larger than the footprint of the p-type TE element, due to the higher thermal conductivity in the n-type material. Therefore, the optimal ratio of footprint areas to achieve the maximum generation and the best cost-efficiency ratio in thermoelectric modules must satisfy that an/Ap < 1, where An and Ap are the footprint areas of the the n-type and p-type junctions, respectively. Brito et al. [49], found that when the thickness of the TE elements is smaller, the electrical resistance is reduced, but this will impact the ΔT of the TE module, because a lower thermal resistance will increase the thermal output and attenuate the temperature difference between the hot and cold sources. However, this will only occur if the usable hot source is low, and the other thermal resistances are high enough to significantly affect the ΔT of the TE module. In their study, Dongxu et al. [38] found that the thickness of the TE legs can be reduced to 1.1 mm, which is 4 mm less than commercial modules, while still achieving the same efficiency. In all these works, simulation tools were successfully used to find the relationships between the different parts of the modules and their respective powers.

2.1.3.4. Useful life

The evolution in the design of TEG modules has also contributed to increasing their useful life. Moreover, the thermal stresses to which the TEG modules are subjected, affect them adversely by the formation of microcracks and the expansion and contraction of TE materials. To address this problem, Skomedal et al. [48] incorporated spring-supported contacts in the legs of TEG modules to dampen thermal expansion and contraction in the modules; these authors concluded that good diffusion barriers and possible coatings can reduce oxidation of the hot side electrodes and interconnections. Likewise, they noted that the TEG module could generate 1 to 3 W/cm2. Furthermore, Ming et al. [79] studied, via numerical analysis, how the non-uniform flow causes the junctions of the TEG modules to be damaged and also decreases their output power. In addition, Merienne et al. [39] investigated the effect of thermal cycles on commercial TEG modules, finding that when rapid temperature changes are applied, their output power can decrease by up to 61%, compared with a module in which the heat flow is constant, and the temperature changes are minimal. Therefore, it is of utmost importance to analyze in detail the design of TEGs and the operating conditions to which they will be subjected in order to establish applications that allow them to extend their useful life.

The current commercial TEG modules have still not reached the economic feasibility, nor the efficiency required for thermal energy recovery applications. Therefore, as mentioned above, the characterization of commercial TEG modules, in the specific conditions to which they are going to

be subjected, requires the use of expensive control equipment, or manual processes, which leads to difficulty in making long-term measurements. Therefore, Elzalik et al. [31] developed a characterization method that allows precise and inexpensive estimation of the maximum power point and the dynamic parameters of the TEG module. The proposed procedure can be used with different sources of residual thermal energy and under different operating conditions.

In relation to the sustainability of TEG modules, authors such as Khanmohammadi et al. [32]and Heber et al. [33] state that the amortization period and the power ratio of commercial TEGs make them not viable to be used exclusively as a generation method. Therefore, they recommend using them as a complement to other methods of recovering residual thermal energy, thus generating an integrated system, or the development of segmented TEG modules that allow greater efficiency and profitability.

2.1.3.5. Thermoelectric Generators

As previously mentioned, the main limitation for the use of TEG is its cost-efficiency ratio; therefore, this type of generator still does not compete with conventional mechanical thermodynamic systems or the electrochemical systems of Rankine, Stirling, Brayton, expansion devices or fuel cells. These types of conventional generation systems have a wide application ranging from heat utilization with a lower output power range to greater than 10 kW. For their part, TE materials are usually utilized for applications with an output power of less than 10 kW [59], which makes them suitable for specific power requirements. Yazawa et al. [65], focused their research on the economic viability that TEGs can achieve with respect to other types of electricity generation systems. The authors found that TEG modules with a ZT of 0.8 can achieve a cost-performance ratio of USD $ 0.86 /W. This makes TEG systems competitive with other power generation systems. It was also found that TEG systems have commercial profitability if they have a cost-performance ratio of less than USD $ 1 /W [42].

In the manufacture of TEG systems, the main component is the TEG module, and the other components such as heat sinks, and supports help the system to perform better. Mori et al. [50] estimated that the TEG modules only represent 60% of the cost of whole systems and focused the design of the system on heat concentration structures that would help to double the efficiency of power generation and that could reduce the total cost in the system by half. Likewise, Hendricks et al. [51] warned that the cost of the heat exchanger, which is the element of the system that most frequently increases the total costs of TEG modules, should be further investigated to achieve profitability of the system.

Lately, the automotive industry has initiated investigations into TEG systems due to the considerable losses of caloric energy that arise from the combustion process, which could be used to power other vehicle systems. Indeed, the incorporation of these energy recovery systems, could significantly reduce CO2 emissions into the atmosphere.

Arsie et al. [55] proposed the incorporation of a TEG system in the exhaust of a car using commercial 14 Hz TEG modules. In their research, the temperature gradient was guaranteed using refrigerant on the cold side of the module; the system was connected directly to the battery and alternator of a

vehicle, and using a longitudinal model, it was possible to determine that the system displaces the energy of the alternator by between 15 and 20%, having an average saving of ~1 g/km of CO2 in standard driving cycles.

Fernández et al. [42] used commercial Bi2Te3 TEG modules for heat recovery from light duty diesel engines as they produce ~386 W of recoverable power under common vehicle driving conditions. In their research they found that in commercial TEG modules, it is only possible to recover about 37.6 W, if no additional improvements, such as advanced heat exchangers, are applied. The authors also found that when a cooling system is able to maintain the cold side of the TEG module at 50 ◦C (less than the engine system coolant temperature), up to 75 W of power can be obtained.

Heber et al. [33] in 2020, manufactured a TEG system for natural gas heavy vehicles, in which they used 168 commercial modules based on SnTe. The cost of the TEG was EUR 1811, and a maximum power of 1507 W was achieved with a power density 50 W/kg, a reduction in CO2 emissions of 4.9 (9.4) g (CO2)/km, and a cost-efficiency ratio of 1.2 EUR/W, which suggests that the system is profitable.

Likewise, the use of TEGs as complementary systems has been investigated to compensate the cost-efficiency ratio in different applications to reduce CO2 emissions. Thus, Bellos et al. [81] investigated the efficiency of a solar energy-induced TEG using commercial Bi2Te3 TEG modules, and carrying out a financial analysis, found that the cost of the investment would be 1 EUR/W, with a payback period of 4.55 years and a leveled cost of electricity of 0.0441 EUR/kWh, indicating that this system would be unprofitable.

2.1.3.6. Sustainability (Circular Economy)

As noted above, commercial TE materials are not yet sufficiently cheap, and high efficiency materials are not yet mass produced. Until now, the most commonly used commercial TE materials are Bi2Te3-based alloys because they have advantages such as easy bulk processing. However, although they are precursors, high energy expenditure and expensive techniques are used in their processing both for power generation and for cooling at temperatures close to ambient levels. On the other hand, TE materials use elements such as bismuth, tellurium, antimony, selenium, and lead, among others, which are expensive, scarce, and sometimes toxic. As mentioned earlier, from the point of view of the circular economy, the recycling of TEG modules could generate great economic benefits since it would allow obtaining raw materials for the manufacture of new TEG modules or other electronic devices, generating a reduction in the consumption of scarce elements. Moreover, they also generate environmental advantages because the improper disposal of these materials is avoided, which can benefit both the environment and human health.

At the time of writing this paper, the scientific publications on recycling TEG modules are still quite sparse. However, currently there are different ways to recycle TEG modules based on tellurium bismuth, from which three approaches can be differentiated based on the separation techniques: (i) chemical, (ii) thermal, and (iii) bacterial methods. On the other hand, in some cases only some parts of the TEG modules are recycled or only the elements of the semiconductors are recovered. According

to the bibliographic review carried out, approaches have been proposed for the recycling of commercial TEG modules based on bismuth tellurium, by taking advantage of the differences in melting temperature of the constituent materials. In this way, the separation of the different constituents of commercial modules (plastics, Cu, Bi2Te3 and Al2O3) in an efficient way might be achieved by mechanical processing which relies on the entropy changes of these materials[30].

The TE materials have been separated by thermal processes followed by chemical separation processes, in which the characterization of the materials of the TE modules was conducted by techniques such as differential scanning calorimetry (DSC), X-ray diffraction (DRX) and field emission scanning electron microscopy (FESEM), which give information on the material types, melting temperatures and the distribution of the materials. This allows their separation based on the differences in thermal and chemical properties. This type of separation is initially carried out by means of thermal treatments such as hot oil baths at 250 ◦C for the removal of solder from the -n (Bi2Te3) and the p-type (Bi0.5Sb1.5Te3) semiconductors. Later they are subjected to a mixed acid solution (HCl and HNO3 in a 3:1 ratio) at room temperature. At this point, the Sb of the semiconductor's precipitates. Then, the solution is then filtered, washed and sintered in order to obtain nano-powders of Bi2Te3 -n type with a particle size of ~15 nm purity [44], [82].

None of the previous works reports a characterization of the thermoelectric properties of the recovered TE materials. The characterization would be of great importance in order to know if the processes used for their separation in any way affect the properties of the recovered products and their possible use in future applications. Table 7 lists some recent works in relation to the final disposal of thermoelectric modules.

Table 7. Bibliographic review of the final disposal of thermoelectric modules in recent years.

Year	Ref	Number of Articles	Country
2020	[83]	1	Finland
2017	[84]	2	France
	[30]		Korea
2014	[47]	1	Korea
2013	[50]	1	Korea

It is clear then that there is a global need for sustainable technologies [85]–[87]and the circularity of materials and processes are areas where TE can have a significant impact as the main, partner, or complementary technology since it is a particularly adaptable technology [88].

2.1.4. Remarks and Conclusions

Between 2010 and 2020, there have been few studies concerning thermoelectric generator (TEG) modules that examine the larger holistic picture from mass manufacturing, profitability (from the economic point of view), efficiency, life cycle, and competitiveness to final disposal. Despite this, in

the systematic search, an approach towards circular economy and sustainability has been considered indirectly since the articles analyzed covered topics ranging from raw thermoelectric TE materials, manufacturing of TEG modules, energy efficiency, and also the applicability and recycling of materials and modules.

The cost of manufacturing the modules is a little explored topic since in most works, only the relationships concerning the cost of the constituent TE materials are analyzed, and other factors that contribute to the high commercial cost of these modules are not examined. In the present review it is highlighted that the efficiency of TEG modules depends, in addition to the TE materials, on external agents such as refrigeration systems, connections between the TEG modules, and the environment in which they will be operated. Therefore, these are important research topics to improve the cost-efficiency ratio of TEG systems.

Modeling is a valuable tool in predicting the efficiency of TEG modules at different stages of their development and implementation. Additionally, the present research evidences the lack of work oriented towards the circular economy and sustainability of TEG modules, highlighting this aspect as an extremely important area for the development of TEG systems.

Taking into account the limitations that current TEG modules present in relation to the efficiency-cost relationship and the lack of research from circular economy and sustainability perspectives, this review proposes an approach for new studies that would allow an improved understanding of the processes used and their useful life. The research approach would aim to balance the cost-efficiency ratio from a sustainability perspective, not only addressing the base material, but also provide a more general approach to understanding the entire life cycle of the modules from their manufacture to their final disposal. This would provide more information on the economic viability and sustainability of TE materials and modules.

2.2. State of Art

The demand for energy worldwide is increasing due to the increase in the economy, the population, the scarcity of this, the cost and pollution generated by the main sources of energy, which are non-renewable resources such as oil, coal, and natural gas; All these factors make the search for new sources of clean and efficient energy more necessary. Although today great potential is seen in wind and solar energy as renewable energy sources, there is also great potential in the recycling of thermal energy that is lost in many industrial processes and in many of the technologies used in everyday life such as cars; Here is one of the relevant applications for the development of efficient thermoelectric materials that allow this thermal energy to be recovered and converted into electrical energy[7], [89]. In addition to being used for the recovery of thermal energy, thermoelectric materials can also be used for the manufacture of cooling systems.[90]

The thermoelectric properties of materials are explained by three main effects, the Seebeck effect, Peltier, and Thomson, which are interrelated and are the basis of the entire theory of thermoelectricity.[91]

The Seebeck effect occurs when between two materials (metals, conductors or semiconductors) an electrical voltage can be generated when they are subjected to a temperature change, the thermoelectric materials that are governed by this effect are used for the recovery of thermal energy. The Seebeck effect (S) is defined by equation (1).

$$S = \frac{\Delta V}{\Delta T} \text{ (1)}$$

Where S is the Seebeck coefficient, ΔV is the voltage change in volts and ΔT is the temperature gradient in K.

The Peltier effect is the opposite phenomenon to the Seebeck, because the materials are subjected to a voltage change and this generates that the ends of the materials increase or decrease the temperature depending on the applied voltage, this type of materials are used for the manufacture of cooling systems. The Peltier coefficient (π) is defined by equation (2).

$$\pi_{AB} = \frac{q}{I} \text{ (2)}$$

Where π_{AB} is the Peltier coefficient, q is the rate of heating or cooling at each junction and I is the electric current.

Finally, the Thomson effect explains that the effects (Seebeck and Peltier effects) can occur reversibly within the same material. The Thomson effect is expressed with the equation.

$$q = \rho J^2 - \sigma J \Delta T \text{ (3)}$$

Where σ is the Thomson coefficient, ρ the resistivity of the material, J the current density, ΔT the temperature gradient y, q is the rate of heating or cooling at each junction.

The figure of dimensionless merit, (ZT) indicates the performance of a thermoelectric material and is expressed by the equation.

$$ZT = \frac{S^2}{K}\sigma T \text{ (4)}$$

Where S is the Seebeck coefficient, σ is the electrical conductivity, K is the thermal conductivity, and T is the absolute temperature.

Having the figure of merit for the thermoelectric material you can know the power conversion efficiency of the device given by the equation:

$$\eta = \frac{\Delta T}{Tcaliente}\frac{\sqrt{1+ZT}-1}{\sqrt{1+ZT}+\frac{Tfrio}{Tcaliente}} \text{(5)}$$

Where ΔT is the temperature gradient with respect to the ends of the device, T is the temperature of the hot and cold end and ZT is the merit figure presented by the material. In Figure 7, the behavior of the efficiency of the thermoelectric devices vs. the temperature for different numbers of merit that the thermoelectric material possesses can be observed Figure 7.

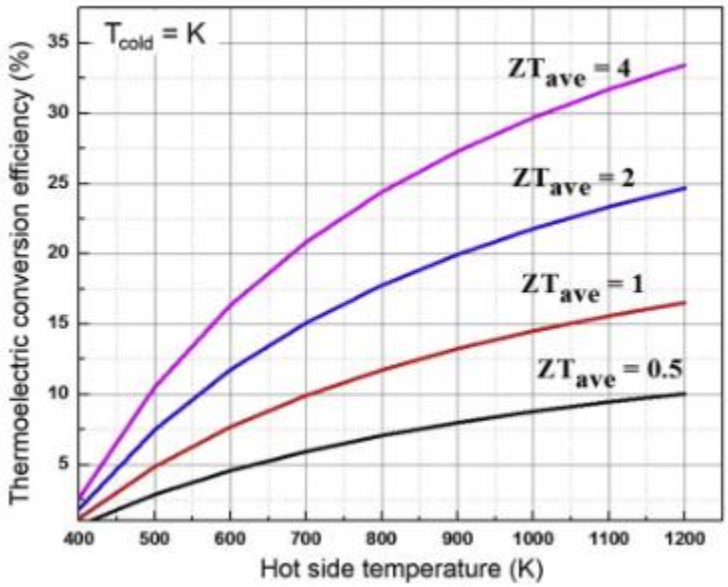

Figure 7. Thermodynamic conversion graph efficiency vs temperature for different ZT values.[92]

2.2.1. Thermoelectrics Bi_2Te_3

Bi_2Te_3 based materials are very versatile because they work at room temperature and have good properties to be used in applications such as cooling, power generation and as a thermal sensor.

The $Bi_2 Te_3$ has a rhombohedral crystal structure which is made up of sets of sequences of quintuple layers of Te-Bi atoms connected by ionic and covalent bonds along the c-axis, the neighboring layers of Te are more weakly connected by Van Der Wals bonds.[91], [93]

The band energy of Bi_2Te_3 is approximately 0.15 eV, being small means that by exciting the material with some type of energy the electrons can jump the energy gap between the valence and conduction bands making this material behave like a semiconductor material[93]

The materials of Bi_2Te_3 are found as p-type materials in which the electrical conduction is given by the number of holes which have positive polarity and type n where the conduction is given by the free electrons and their polarity is negative. The investigation of thermoelectric materials based on Bi_2Te_3 both type p and type n are of equal importance because the devices or cells commercially known as Peltier cells, used for different applications require both for their operation. In these cells the semiconductor elements are arranged electrically in series and thermally in parallel.

The implementation of this type of thermoelectric cells for power generation and cooling applications, in most cases is initially sought to obtain predictions of the performance of these and optimal conditions of temperature and geometry in which it will present the best performance in an exact and reliable way, for which mathematical simulation tools are used to manufacture or design these materials.[94]–[99]

At present, it seeks to improve the performance of thermoelectric materials so that they are competitive and efficient, therefore, materials are investigated in which the Seebeck coefficient and electrical conductivity are high, but at the same time it is sought that the thermal conductivity is low. To achieve this there are different research approaches such as nano-structuring[12], [100]–[102], Band Engineering electrónica[93], Quantum confinement[101], [103]–[105], Strategies such as crystal electron crystal phonon glass[82], doping[16], [22], [93], and introduction of defects[106]–[108], Among others, from which the increase in the performance of thermoelectric materials is sought, favoring the transport of electrons, which are respectively involved with the electrical conductivity presented by the material and minimizing the transport of phonons that are mainly the most involved in the transport of heat within the material.

For thermoelectric materials to compete with traditional energy techniques, a ZT close to or greater than 3 must be reached and must be able to withstand the different temperatures to which they may be exposed, so the introduction of different technologies to increase ZT generate that the development of this type of materials is expensive, Many times, their mass production is inefficient, consequently one of the most important challenges is the development of efficient and economically accessible thermoelectric materials.

¡Error! No se encuentra el origen de la referencia.shows some of the materials that have been used as dopants to improve the thermoelectric properties of Bi $_2$Te$_3$ base materials and their respective processing. In this it can be observed that the addiction of materials such as Lutetium[109], Copper[110], zinc oxide[17], and graphene[111], improvements of the figure of merit in the Bi_2Te_3. In the case of graphite, it was found that the addition of 0.05% by weight of graphite without texture improves the ZT of the base material up to 35% reaching a ZT ~ 1.05 at 320K.

Table 8. Doping materials for base thermoelectric material Bi_2Te_3.

Doping	ZT	Temperature (K)	Type	Process
Mg→$Mg_{0.01}Bi_{1.99}Te_3$	~0.8	350	n	Solid state melting method + grinding + cold pressing + spark plasma sintering
Sr→$Sr_{0.01}Bi_{1.99}Te_3$	~0.58	325	n	
Ba→$Ba_{0.01}Bi_{1.99}Te_3$	~0.58	325	n	
Ca→ $Ba_{0.01}Bi_{1.99}Te_3$	~0.2	325	n	
I→ $Bi_2Te_{2.9}I_{0.1}$	~1.1	448	n	Hydrothermal method + hot pressing
Lu→ $Bi_{1.9}Lu_{0.1}Te_3$	~1.7	373	n	
	~0.9	450	n	Microwave-thermal solvent method + spark plasma sintering
Tm→ $Bi_{1.9}Tm_{0.1}Te_3$	~0.7	450	n	

Pb→$Bi_{1.95}Pb_{0.05}Te_3$	~0.63	386	p	Solid state melting method + grinding + hot pressing
Ge→ $Bi_{1.95}Pb_{0.05}Te_3$	~0.95	300	p	Solid state melting method + cold pressing + annealing
Cu →15.6 %Cu-Bi2Te3	~0.67	415	-	Redox reaction + spark plasma sintering
Cu→ 2% Cu-$Bi_{0.5}Sb_{1.5}Te_3$	~1.34	400	p	Fusion spinning method
Cu→ $Cu_{0.01}Bi_{0.48}Sb_{1.52}Te_3$	~1.1	400	p	Solid state melting + grinding + hot pressing
ZnO→ $Bi_{0.4}Sb_{1.6}Te_3$-ZnO	~1.5	329-360	p	Atomic layer deposition + sintering technique
In + 0.25% SbI_3 →$Bi_{1.85}$in 0.15 Te_2Se + 0.25 by weight % SbI3	~1.1	625	n	Solid state melting + hot deformation
Graphene→ $Bi_{0.4}Sb_{1.6}Te_3$+ 0.5% Graphene	~1.26	423	p	High pressure and high temperature synthesis + high pressure sintering
Graphene → $(Bi2Te_3)_{0.2}(Sb_2Te_3)_{0.8+}$ $_{0.4}$% vol Graphene	~1.54	440	p	Solid state melting + grinding + vacuum hot pressing
Graphene → $(Bi2Te_3)_{0.2}(Sb_2Te$ $3)_{0.8+\ 0.3}$% vol Graphene	~1.29	300	p	Solid state melting + grinding + vacuum hot pressing
Graphene→ $Bi_{0.4}\ Sb_{1.6}\ Te_3$+ 0.05% by weight graphene	~1.26	423	p	High Pressure High Temperature (HPHT) Synthesis + Grinding + High Pressure Sintering
Graphite→ $Bi_{0.5}Sb_{1.5}Te_3$+0.05% by weight of graphite	~ 1.05	320	P	powder metallurgy + cold pressing +annealing treatments

2.3. Graphite nanoplatelets

As mentioned above, carbon-based materials have been used to improve thermoelectric properties by working as barriers in the passage of phonons, thus reducing thermal conductivity without negatively affecting the electrical conductivity of the material, generating more efficient materials. Graphite nanoplatelets consist of small graphene stacks and generally have a thickness of 1 to 15 nm, depending on the number of layers, the degree of crystallinity and aspect ratio are their thermal, electrical and mechanical properties.[28], [112]

Graphite nanoplatelets have been used to improve the mechanical, thermal, electrical, electrochemical properties of polymeric, metallic and construction materials[25]–[27], therefore, it is of interest for this work to study the behavior that it presents in the physicochemical and thermoelectric properties of the base material Bi2Te3 through an economical manufacturing method such as powder metallurgy.

CHAPTER 3

3. Materials and Methodology Composite material

3.1. Composite material

3.1.1. Materials

The purity P-Type Bismuth telluride powder (P Type-BiTe) 99.99% from the supplier Wuhan Xinrong New Materials Co of China and graphite nanoplatelets (GNP) (CAS# Grapite 7782-42-5 CAS# Carbon 7740-44-0) from the supplier The Asbury Graphite Mills.INC. was used as thermoelectric base material.

3.1.2. Methodology

3.1.2.1. Manufacture of composite material

Four mixtures were made in order to analyze the behavior of the purity P-Type Bismuth telluride powder (**P Type-BiTe**) thermoelectric material by adding 0, 0.1, 0.5, and 1% wt of graphite nanoplatelets (**GNP).** As received, the P Type-BiTe was mixed with the nanoplatelets in a planetary stainless steel mill with 3 mm balls, it was worked under nitrogen atmosphere in a BMR 10:1 for 3h. To avoid the agglomeration of dusts, stearic acid was used as a process control agent (PCA) in a percentage of 2%wt. The resulting powders were cold compacted under a uniaxial pressure of 32 MPa and the resulting parts were sintered under controlled atmosphere at 200 ° C for 5 h.

Table 9. Design of experiments thermoelectric material.

SAMPLE	0%wt GPN	0.1%wt GPN	0.5%wt GPN	1%wt GPN
% GRAPHITE NANOPLATELETS	0.0%	0.1%	0.5%	1%
% TYPE P BISMUTH TELLURIUM	100.0%	99.9%	99.5%	99.0%

The diagram in the Figure 8, shows all the steps taken for the manufacture of the base material p-type BiTe with x% wt GNP (0, 0.1, 0.5 and 1%). It should be noted that during the storage, grinding and sintering processes were carried out under a controlled nitrogen atmosphere. The only process in which no controlled atmosphere was used was in the process of compaction of cold uniaxial pressing

of ground powders, therefore, by the methods of SEM -EDS and XRD it was required to verify if the samples presented any indication of oxidation.

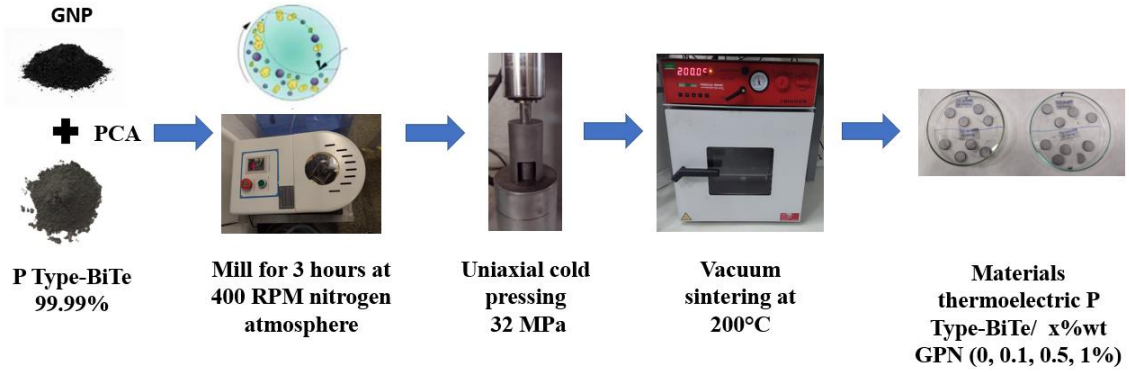

Figure 8. Diagram of the manufacturing process of the composite material p-type BiTe/ x% wt GNP (0, 0.1, 0.5 and 1% wt)

3.1.2.2. Characterization of composite material

For the morphological and mineralogical characterization of the base materials, the powders of the mixtures after grinding and of the compacted and sintered samples, a scanning electron microscope (SEM) reference JEOL JSM – 6490 was used to observe the morphology and a Rigaku MiniFlex 600 diffractometer, in which a sweep between $2\theta = 5°$ and 60° at a step of 0.01° was used, and a velocity of 0.03°/min using a radiation of Cu (λ= 1.5405 Å), with a voltage of 40 kV and a current of 15 mA for mineralogical analysis by X-ray diffraction.

The analysis of the thermoelectric properties of the compacted and sintered samples (bulk composite material) was used thermoelectric property analyzer reference HCS-1 LINSEIS GMBH, with which Measurement of electrical resistivity, coefficient Hall, mobility and Seebeck coefficient were measured.

Density tests were simply measured on 3 samples, weighting them, and using their dimensions measured for this estimate.

CHAPTER 4

4. Raw Materials Characterization

The purity P-Type Bismuth telluride powder (P type-BiTe) 99.99% material supplied by the supplier Wuhan Xinrong New Materials Co of China and the graphite nanoplatelets (GNP) (CAS# Grapite 7782-42-5 CAS# Carbon 7740-44-0) from the supplier The Asbury Graphite Mills.INC was analyzed by scanning electron microscopy (SEM) JEOL JSM 6700R in a high vacuum mode, the powders were placed on a carbon tape, and as the samples were conductive, they were not required to be coated with Au. The crystal structure was identified by X-ray diffraction (XRD), performed on a Rigaku MiniFlex 600 diffractometer, in which a sweep between $2\theta = 5°$ and 60° at a step of 0.01° and a velocity of 0.03 ° / min using a radiation of Cu ($\lambda = 1.5405$ Å), with a voltage of 40 kV and a current of 15 mA the software used for the identification of the peaks was High Score Plus of Malvern Panalytical.

4.1. P-Type Bismuth telluride powder (P Type-BiTe) Characterization

4.1.1. Results Scanning Electron Microscopy

In the Figure 9, the micrograph of the P-Type Bismuth telluride powder is observed in which a highly irregular particle size distribution is observed, and particle agglomerations are observed in some areas, some nanometric grade particles are also observed.

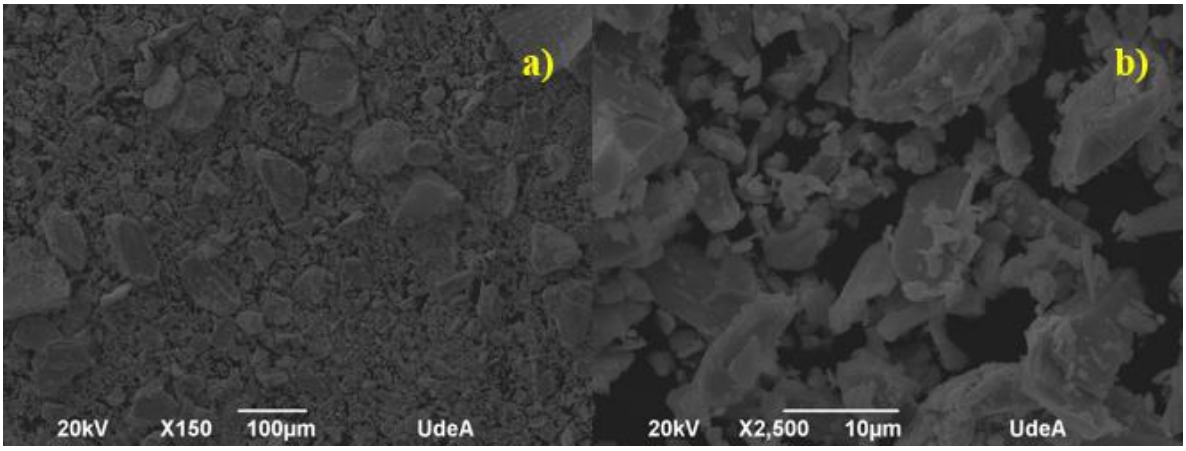

Figure 9. SEM analysis P-Type Bismuth telluride powder (P Type-Bite) 99.99% with magnification a) X 150 b) X2,500

Using the Image J program, the particle distribution was carried out,Figure 10 is observed that the P-Type Bismuth telluride powder (P Type-BiTe) 99.99% has a non-uniform particle size, and the average size is 3,82 μm.

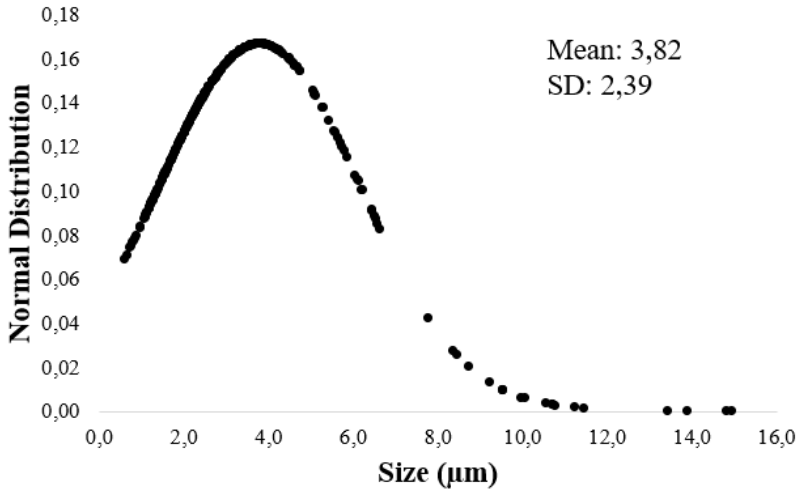

Figure 10. Particle size distribution of P-Type Bismuth telluride powder (P Type-BiTe) 99.99%

4.1.2. Results of XRD

Figure 11 shows the XRD spectrum for the P-Type Bismuth telluride powder 99.99%. All major diffraction peaks match the standard $Bi_{0.5}Sb_{1.5}Te_3$ card ref 00-049-1713 with rhombohedral structure (crystalline group R3m). The peaks found also coincide with those detected in the reviewed literature [113]

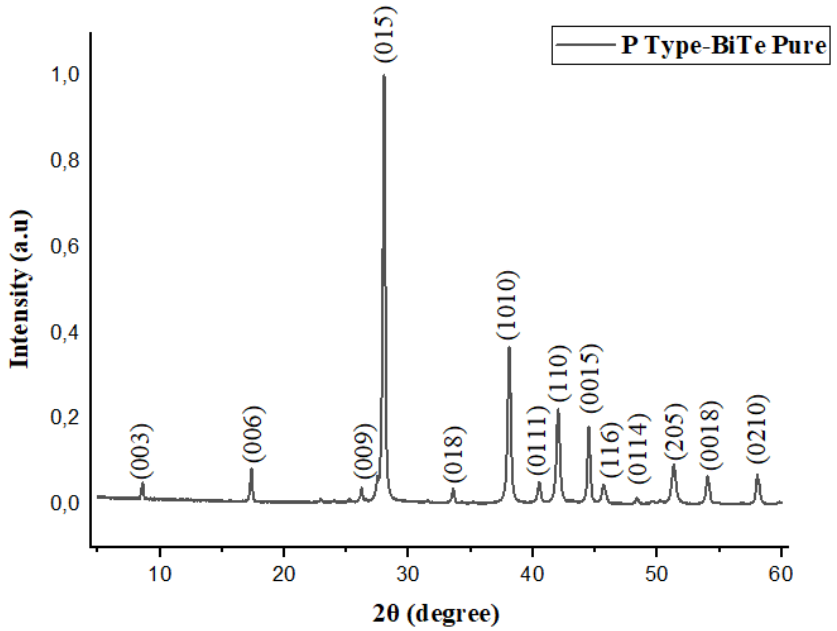

Figure 11. XRD for P-Type Bismuth telluride powder (P type-BiTe) 99.99%

4.2. Graphite nanoplatelets (GNP) Characterization

4.2.1. Results Scanning Electron Microscopy

In the micrograph of the Figure 12 , GNP graphite nanoplatelets are observed in different orientations, some areas of agglomeration are also observed.

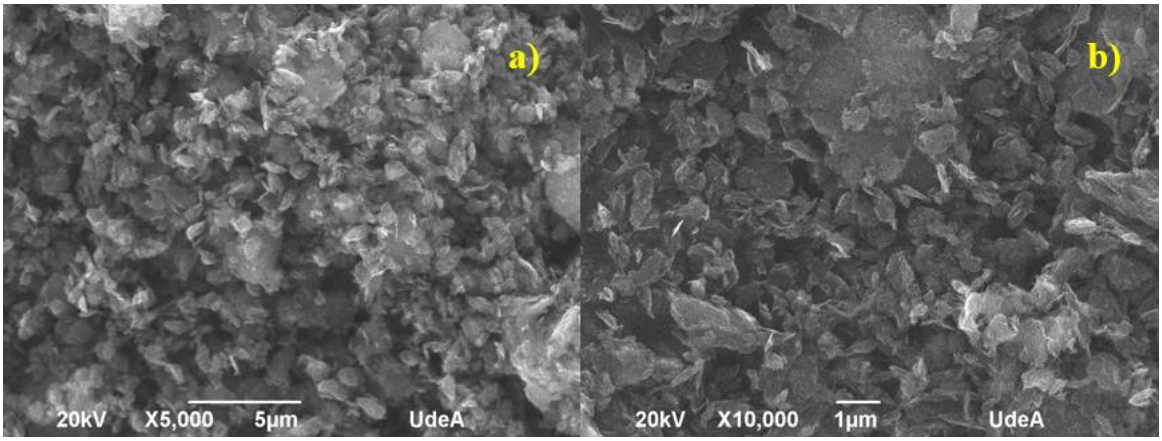

Figure 12. SEM analysis Graphite nanoplatelets (GNP) with magnification a) X 5,000 b) X10,000

In **¡Error! No se encuentra el origen de la referencia.**, a more uniform particle distribution for graphite nanoplatelets and an average size of 0,40 µm.

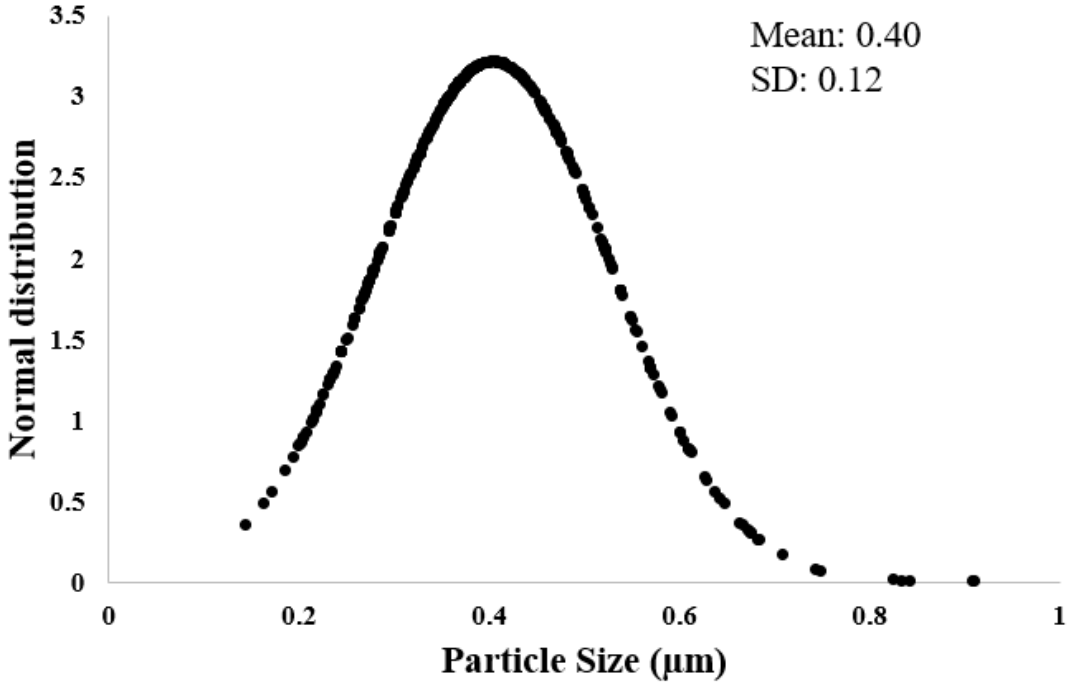

Figure 13. Particle size distribution of Graphite nanoplatelets (GNP)

4.2.2. XRD results

Figure 14, shows the diffractogram of graphite nanoplatelets (GNP). All major diffraction peaks match the standard graphite card Ref. 96-901-1578.

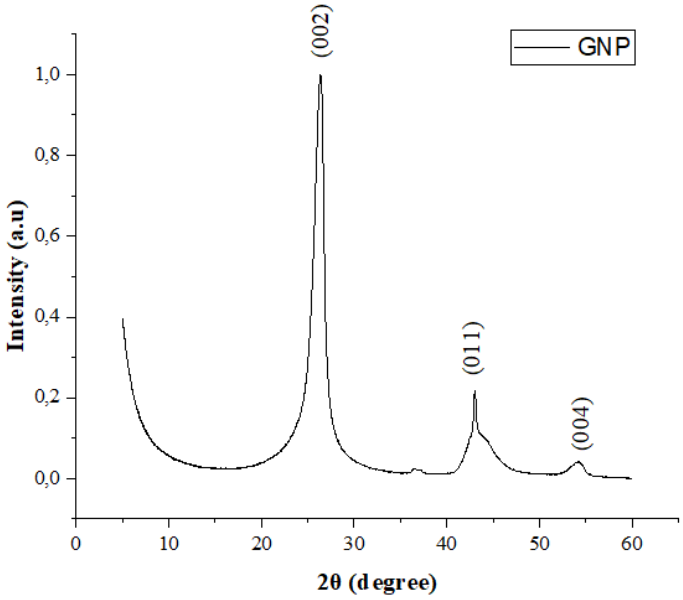

Figure 14. XRD for Graphite nanoplatelets (GNP)

CHAPTER 5

5. Manufacture and Characterization of composite Material

During the manufacture of the composite material, Scanning Electron Microscopy (SEM) and X-ray diffraction (XRD) tests were performed on the powders after grinding and on the bulk material after forming and sintering. To know if the material suffered some oxidation due the cold uniaxial pressing process without a controlled atmosphere, EDS / SEM was performed on the bulk material to know the percentages of oxygen in the samples. Finally, the manufactured bulk materials were densely tested, and their thermoelectric properties were characterized.

5.1. Characterization of milled composite material.

5.1.1. Scanning Electron Microscopy Results

Figure 15, **¡Error! No se encuentra el origen de la referencia.**, Figure 19 and Figure 21, show the micrographs of the powder of the composite material 0%wt GNP, 0.1%wt GNP, 0.5%wt GNP, 1%wt GNP respectively after milling, we can see that the typical micrographs of BiTe base composite powders with the allotropic forms of carbon such as graphite. It can be observed in the micrographs that by increasing the percentage of graphite nanoplatelets in the larger particles that can be attributed

to the P-type BiTe smaller particles are deposited, these small particles can be contributed to graphite nanoplatelets due to the difference in initial size and that this phenomenon is more evident in the micrograph Figure 21, for composite material in powder p-type BiTe with 1% wt GNP.

For the material with 0%wt GNP in the micrograph of the **Figure 15** smaller particles are observed and evaluating both the micrographs and the particle distribution of the **¡Error! No se encuentra el origen de la referencia.** for this specimen it is obtained that the particle size of the material after 3 hours of grinding at 400 RPM decreased by approximately 60.12% with respect to the base material acquired (see Figure 9 and Figure 10).

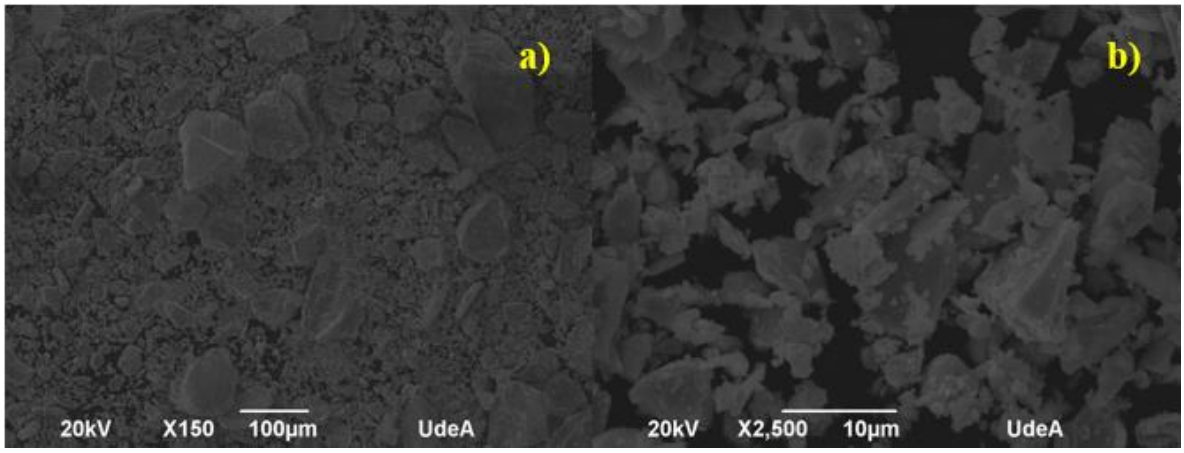

Figure 15. SEM analysis for composite material in powder p-type BiTe with 0% wt GNP with magnification a) X 150 b) X2,500

¡Error! No se encuentra el origen de la referencia., shows the particle distribution for the composite material in powder p-type BiTe with 0% wt GNP and obtained an average particle size of 2.29 µm.

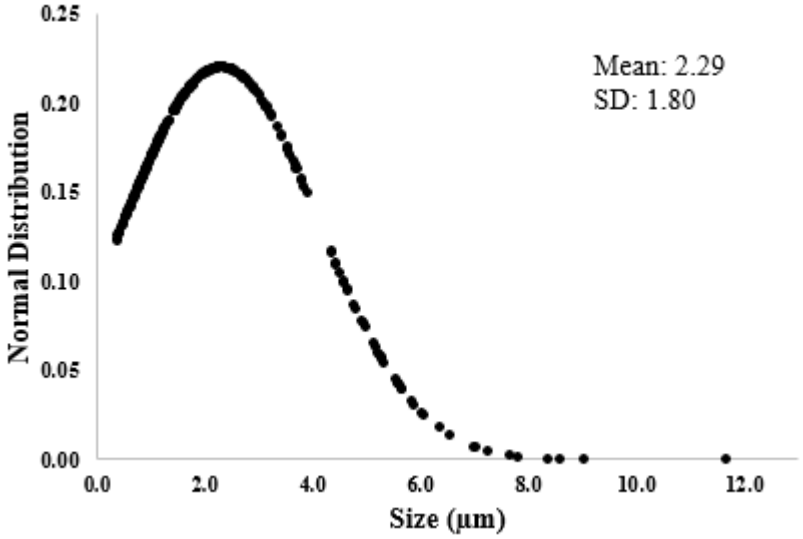

Figure 16. Particle size distribution of composite material in powder p-type BiTe with 0% wt GNP.

In the micrograph of **¡Error! No se encuentra el origen de la referencia.**, for composite material in powder p-type BiTe with 0.1% wt GNP, we can observe small particles on the surface of the particles of p-type BiTe can be to graphite nanoplatelets the GNP.

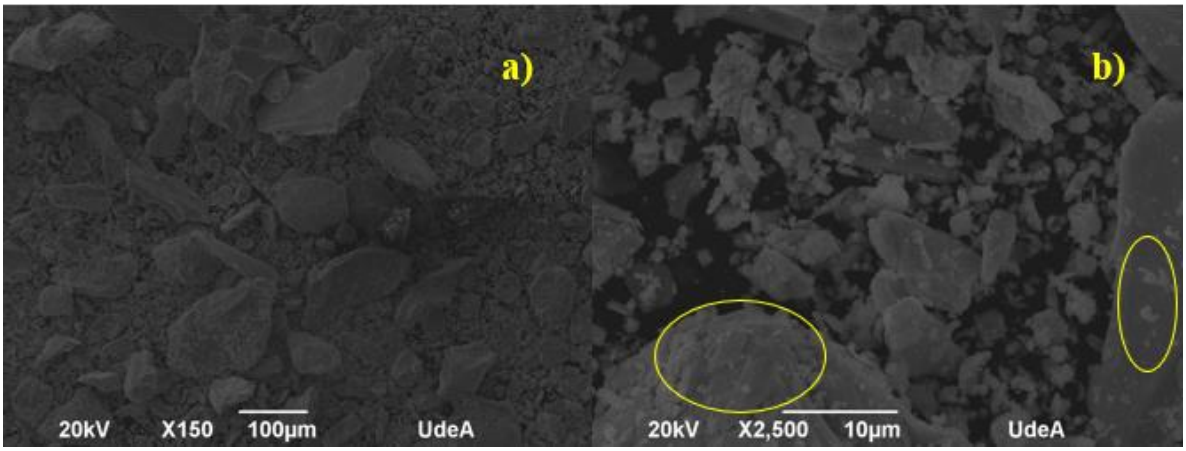

Figure 17. SEM analysis for composite material in powder p-type BiTe with 0.1% wt GNP with magnification a) X 150 b) X2,500.

¡Error! No se encuentra el origen de la referencia., shows the particle distribution for the composite material in powder p-type BiTe with 0,1% wt GNP and obtained an average particle size of 1,62 µm. a higher concentration of particles between 0 and 3 µm is observed, which indicates a greater number of small particles due to the incorporation of graphite nanoplatelets to the base material.

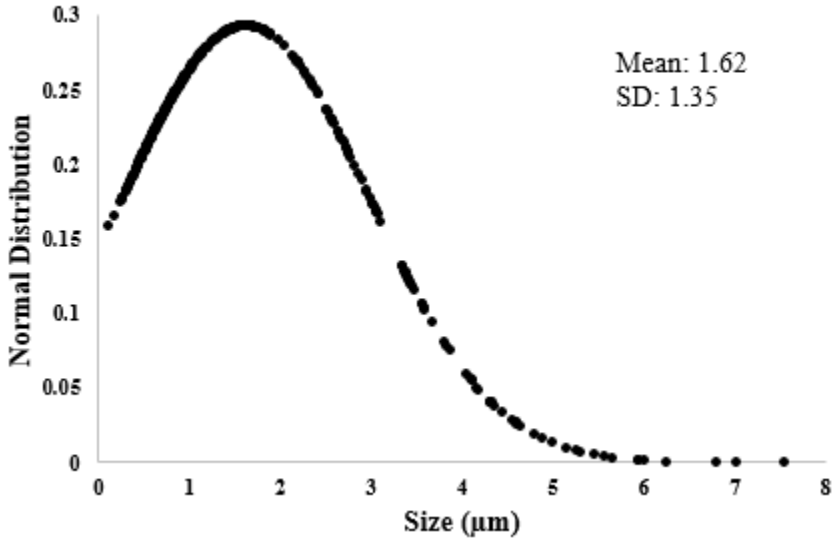

Figure 18. Particle size distribution of composite material in powder p-type BiTe with 0,1%wt GNP.

In the area used for the SEM analysis of material for thermoelectric in powder p-type BiTe with 0.5% wt GNP (see Figure 19), we can observe some agglomerations of graphite nanoplatelets, but the micrograph with magnification X 2,500 we observed mostly the particles of p-type BiTe, despite this an average particle size of 2.08 µm was obtained, which is smaller than that obtained in the sample of 0%wt GNP.

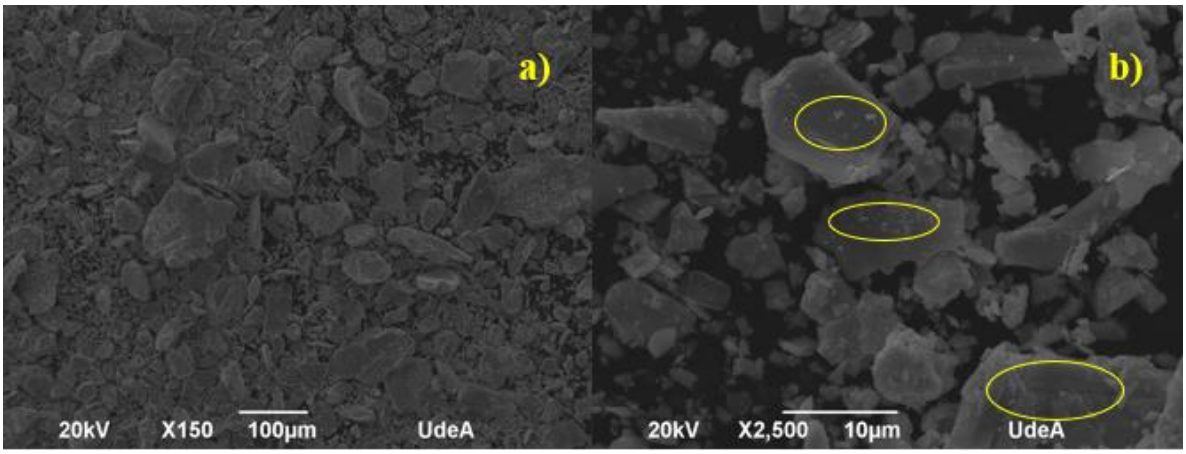

Figure 19. SEM analysis for material Thermoelectric in powder p-type BiTe with 0.5% wt GNP with magnification a) X 150 b) X2,500

¡Error! No se encuentra el origen de la referencia., shows the particle distribution for the composite material in powder p-type BiTe with 0,5% wt GNP and obtained an average particle size of 2,08 µm.

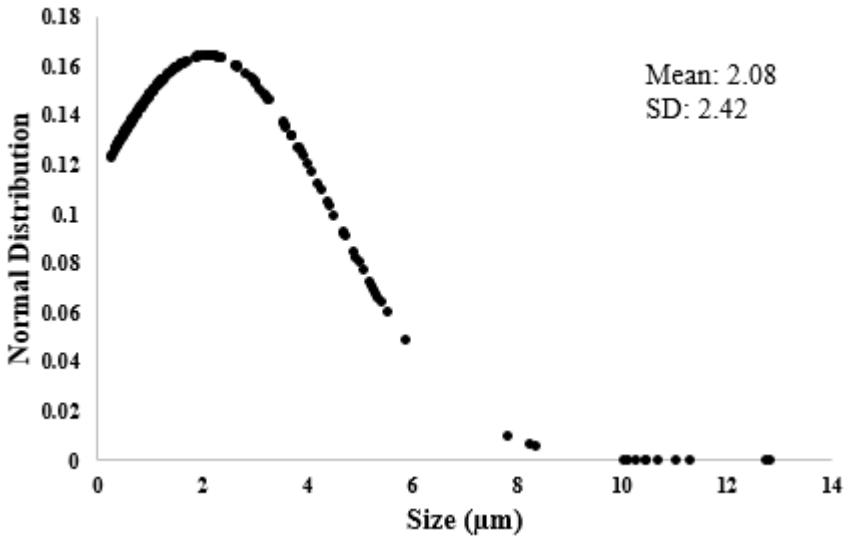

Figure 20. Particle size distribution of composite material in powder p-type BiTe with 0,5%wt GNP

Figure 21, shows the micrographs for composite material in powder p-type BiTe with 1% wt GNP, in these are more evident the agglomerations of graphite nanoplatelets on the surface of the particles of p- type BiTe and analyzing the particle distribution (see **¡Error! No se encuentra el origen de la**

referencia.) an average size of 1.21 μm was obtained due to the increase in the content of graphite nanoplatelets.

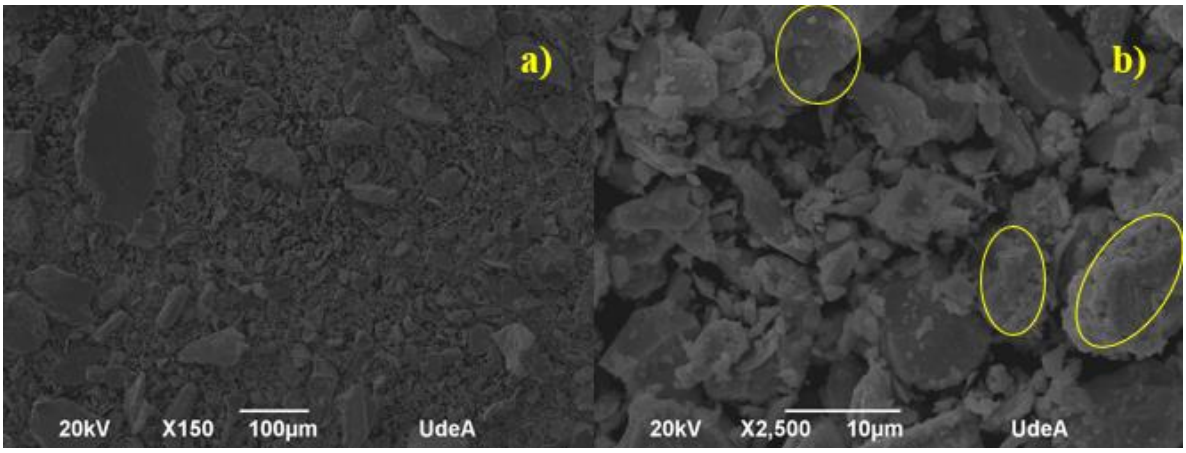

Figure 21. SEM analysis for composite material in powder p-type BiTe with 1% wt GNP with magnification a) X 150 b) X2,500

¡Error! No se encuentra el origen de la referencia., shows the particle distribution for the composite material in powder p-type BiTe with 1% wt GNP and obtained an average particle size of 1,21 μm.

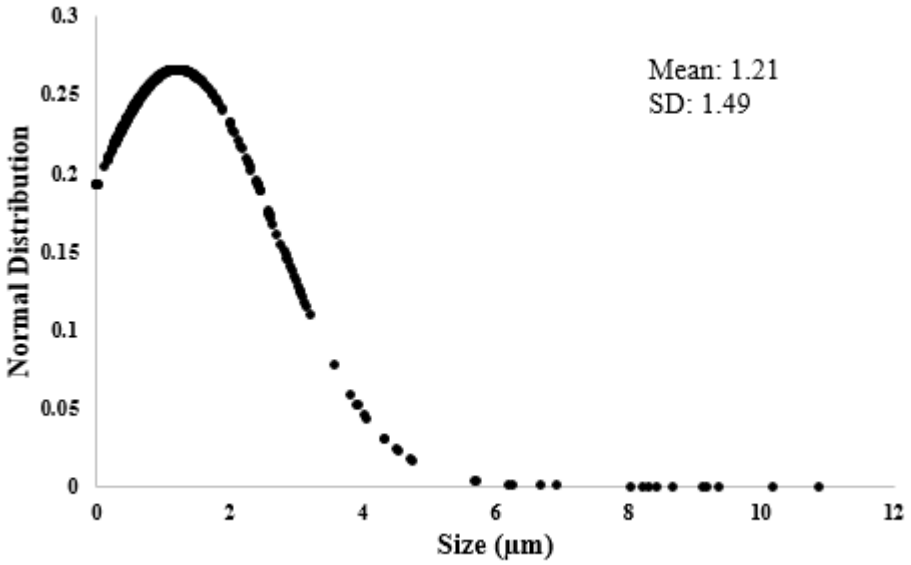

Figure 22. Particle size distribution of composite material in powder p-type BiTe with 1%wt GNP

5.1.2. Results of XRD

In the XRD Figure 23 results all samples correspond to the main peaks for Bismuth Antimony Telluride (Bi0.5Sb1.5Te3 Ref. 00-049-1713), it is observed that the intensity of peaks 009, 0015 and 0018 intensifies with increasing percentage of GNP and correspond to peaks 002, 011 and 004 of GNP respectively (see Figure 14).

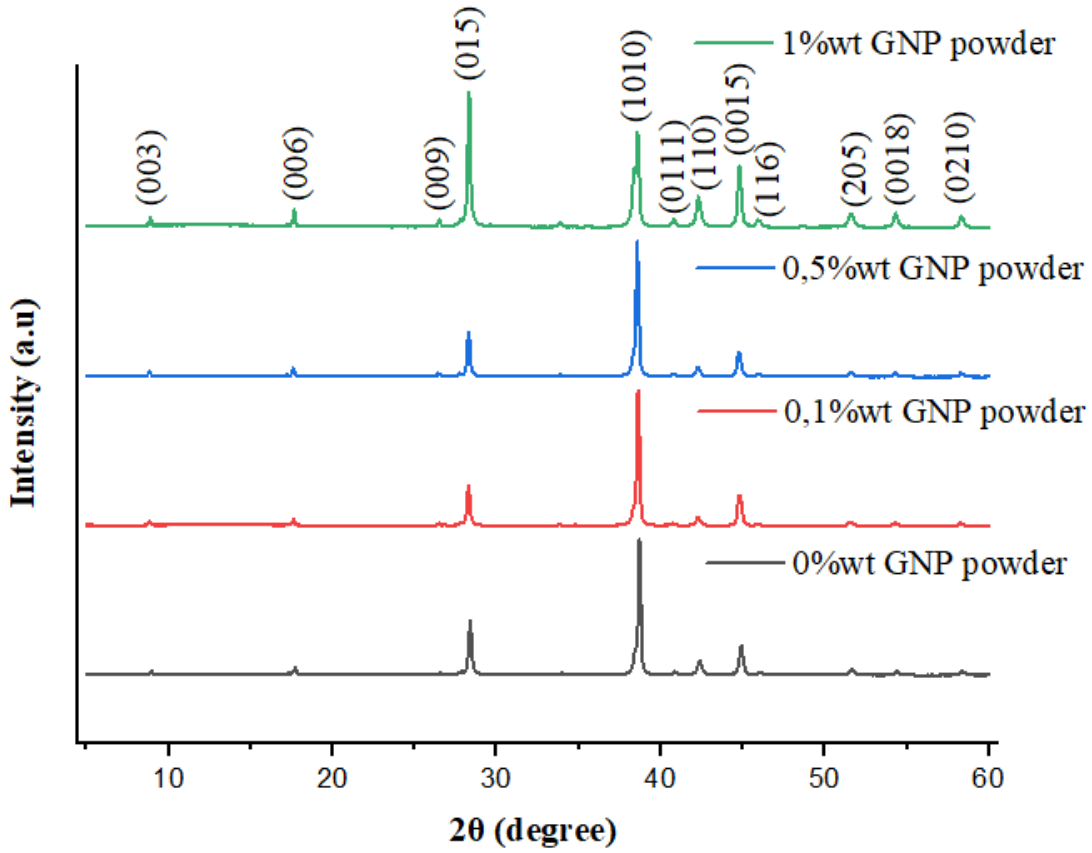

Figure 23. XRD for composite material in powder p-type BiTe with 0, 0.1, 0.5 and 1% wt GNP.

5.2. Characterization of the composite material bulk

5.2.1. Results Scanning Electron Microscopy with EDS

In the Figure 24, Figure 25, Figure 26, Figure 27, the SEM micrographics and EDS analysis of the p-type BiTe composite materials with 0, 0.1, 0.5 and 1% wt GNP are presented, cold compacted at 32 MPa without controlled atmosphere and sintered under vacuum at 200 ° C for 5 hours. Table 10, shows the composition obtained for the composite material in powder p-type BiTe with 0, 0.1, 0.5 and 1% wt GNP. The samples were previously polished in a drybox and subjected to sonication in methanol for 30 minutes.

The micrograph Figure 24 a) and b) for the composite material p-type BiTe with 0% wt GNP can be seen the typical grains for the p-type BiTe. In Figure 24 c) and Table 10 corresponding to the EDS analysis of the material, the peaks of Bi, Te and Sb are observed, but there is also a peak of oxygen (1,96% wt)that was expected to present oxidation because in the pressing process the powders and the compacted sample were exposed to an uncontrolled atmosphere. An unusual peak of carbon is also observed, and, in this sample, GNP was not used, this can be attributed to the use of stearic acid (C18H36O2) as PCA and the incorrect elimination in the sintering of the material.

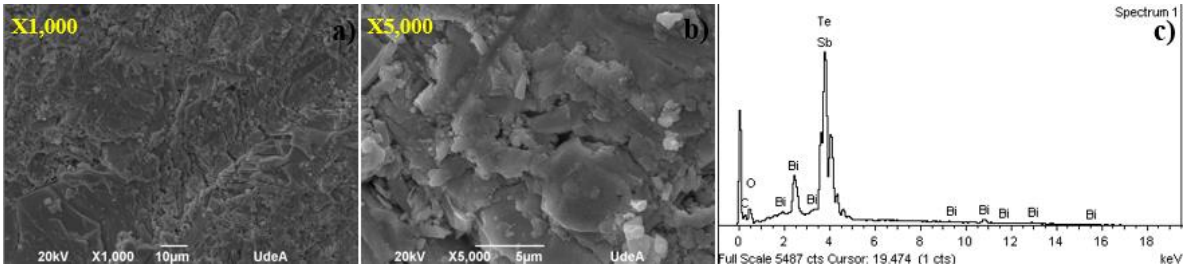

Figure 24. SEM analysis for composite material bulk p-type BiTe with 0% wt GNP with magnification a) X 1,000 b) X5,000 and c) EDS.

In Figure 25, Figure 26 y Figure 27, we can see that for the composite material p-type BiTe with 0.1, 0.5 and 1%wt GNP areas with agglomerations are seen and, in the EDS, results the peaks of Bi, Te and Sb of the base material and C of the GNP are observed.

Figure 25 c) the oxidation of the material is also manifested by the peak of the EDS spectrum and the composition results in which there is 1.24 % wt of oxygen in the sample (see Table 10)

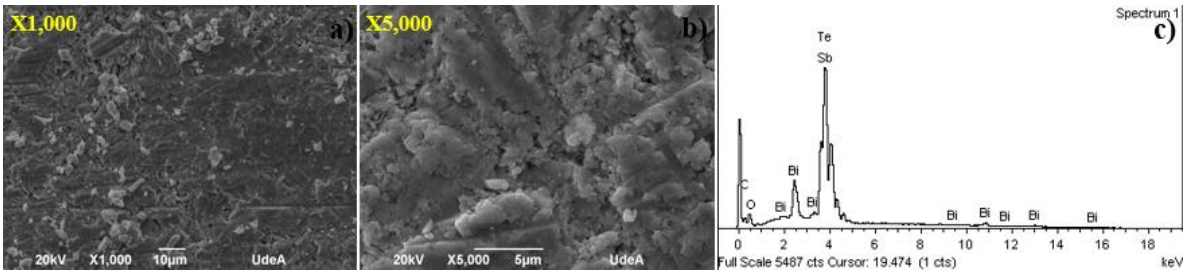

Figure 25. SEM analysis for composite material bulk p-type BiTe with 0.1% wt GNP with magnification a) X1,000 b) X5,000 and c) EDS.

In Figure 26 c), we can see in the spectrum of EDS for composite material p-type BiTe with 0.1%wt GNP the presence of oxygen, verifying in Table 10 there is a 1.68% wt of oxygen in the sample.

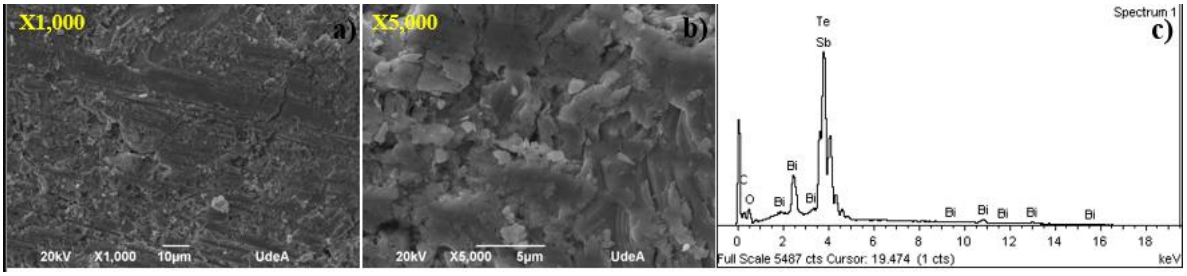

Figure 26. SEM analysis for composite material bulk p-type BiTe with 0.5% wt GNP with magnification a) X1,000 b) X5,000 and c) EDS.

For the composite material bulk p-type BiTe with 1% wt GNP, was the sample with the lowest percentage of oxygen in its composition with 0.96%wt O (see Table 10)

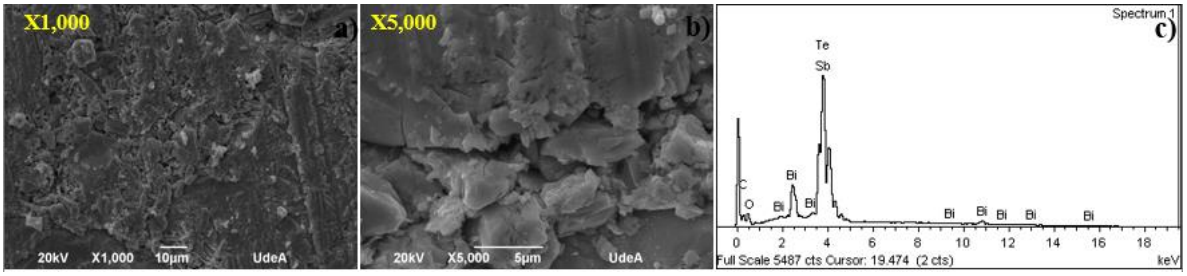

Figure 27. SEM analysis for composite material bulk p-type BiTe with 1% wt GNP.

In the EDS analysis (see **Table 10**), oxygen content could be observed in all bulk samples, which indicates oxidation during the manufacturing process of thermoelectric materials, which can affect their thermoelectric properties [114].

Table 10. Composition obtained by EDS for composite material in powder p-type BiTe with 0, 0.1, 0.5 and 1% wt GNP.

	Element	C	O	Sb	Te	Bi
0%WT GNP BULK	**(weight %)**	2,43	1,96	25,39	57,7	12,52
0,1%WT GNP BULK	**(weight %)**	2,50	1,24	26,42	56,76	13,09
0,5%WT GNP BULK	**(weight %)**	3,51	1,68	26,24	55,77	12,79
1%WT GNP BULK	**(weight %)**	3,89	0,92	26,43	56,41	12,35

5.2.2. Results of XRD

In the Figure 28, the results of XRD for composite material bulk p-type BiTe with 0, 0.1, 0.5 and 1% wt GNP. In the spectra it is observed that the peaks coincide again with the main peaks for Bismuth Antimony Tellurude (Bi0.5Sb1.5Te3 Ref. 00-049-1713), in this case, in the peaks associated with graphite there are no changes in the intensity of the peaks between each sample.

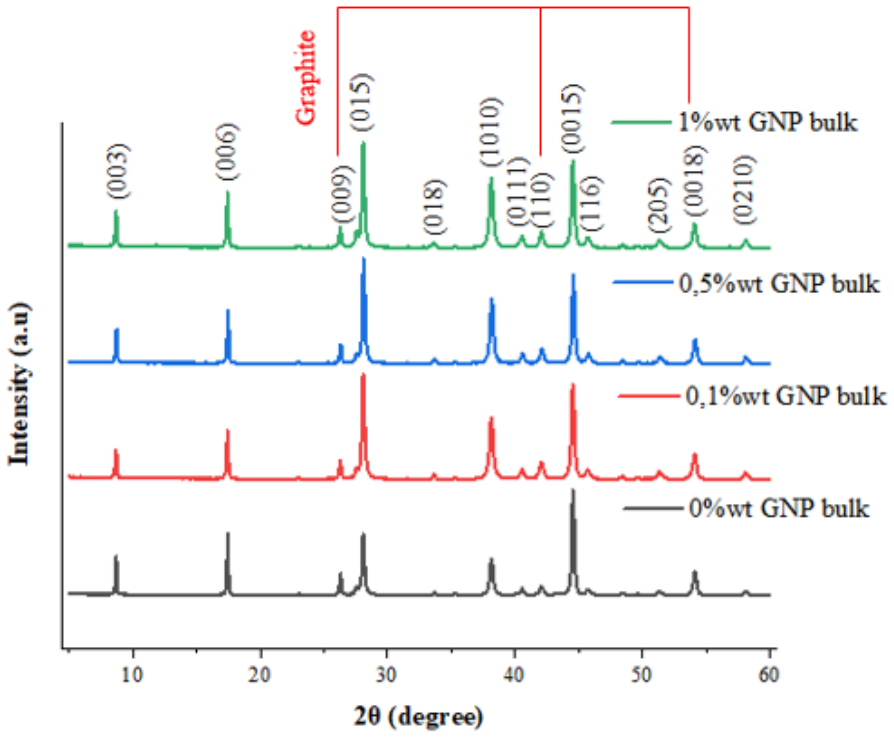

Figure 28. XRD for composite material bulk p-type BiTe with 0, 0.1, 0.5 and 1% wt GNP.

5.2.3. Density

The density was determined by the dimensional method, in which with the help of a Vernier caliber the height and diameter measurements of the specimens were taken. To obtain the weight of the specimens, a high precision balance was used. In the Figure 29. Density for composite material bulk p-type BiTe with 0, 0.1, 0.5 and 1% wt GNP. you can see the results obtained for each sample. It can be observed that the density increases slightly by adding the graphite nanoplatelets to the base material P Type BiTe. The density of bulk samples is: 4.76, 4.78, 5.12, 5.16 g/cm3 for 0%wt GNP, 0.1% wt GNP, 0.5%wt GNP and 1%wt GNP respectively.

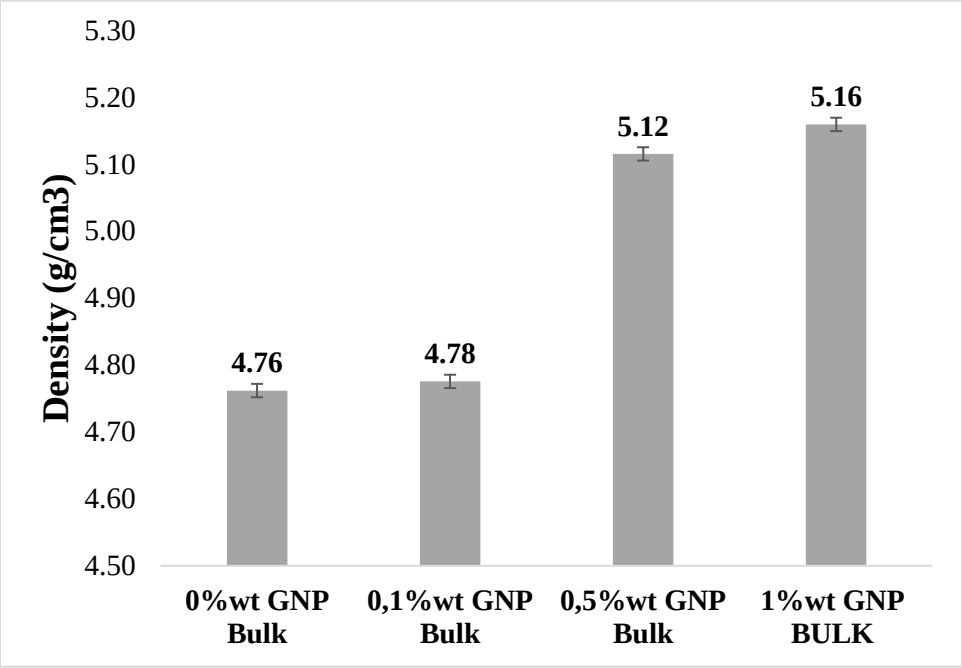

Figure 29. Density for composite material bulk p-type BiTe with 0, 0.1, 0.5 and 1% wt GNP.

5.2.4. Results of the characterization of thermoelectric properties

The thermoelectric properties of electrical conductivity, mobility and Seebeck coefficient for bulk composite materials p-type BiTe with 0, 0.1, 0.5, and 1% wt GNP were measured with the thermoelectric property's analyzer HCS-1 LINSEIS GMBH, the tests were performed in an uncontrolled atmosphere, and two sensors were used, the first to measure electrical conductivity, Hall coefficient, Hall mobility in a temperature range between 300-470K under ASTM F76 – 08 and the second to measure the Seebeck coefficient in a temperature range between 300-420K

The thermal conductivity was calculated with the law of conductivity of Wiedemann Franz, which establishes for metals the ratio of the electronic contribution of thermal conductivity to electrical conductivity [115]–[117]:

$$\frac{k}{\sigma} = LT \ (1)$$

Donde σ es la conductividad eléctrica(S/m); k la conductividad térmica (W/mK); y L es el número de Lorenz ($2{,}44x10^{-8}$ $W\Omega/K^2$) y T es la temperatura absoluta.

Figure 30. shows the behavior of electrical conductivities for composite material bulk p-type BiTe with 0, 0.1, 0.5, and 1% wt GNP. The figure indicates that increasing the percentage of graphite nanoplatelets also decreases the material's electrical conductivity except for the compound with 1% wt. The material with the lowest electrical conductivity was the bulk p-type BiTe with 0.5%wt GNP. When analyzing each of the compositions independently, the electrical conductivity in each tends to decrease with increasing temperature a typical feature of thermoelectric materials.

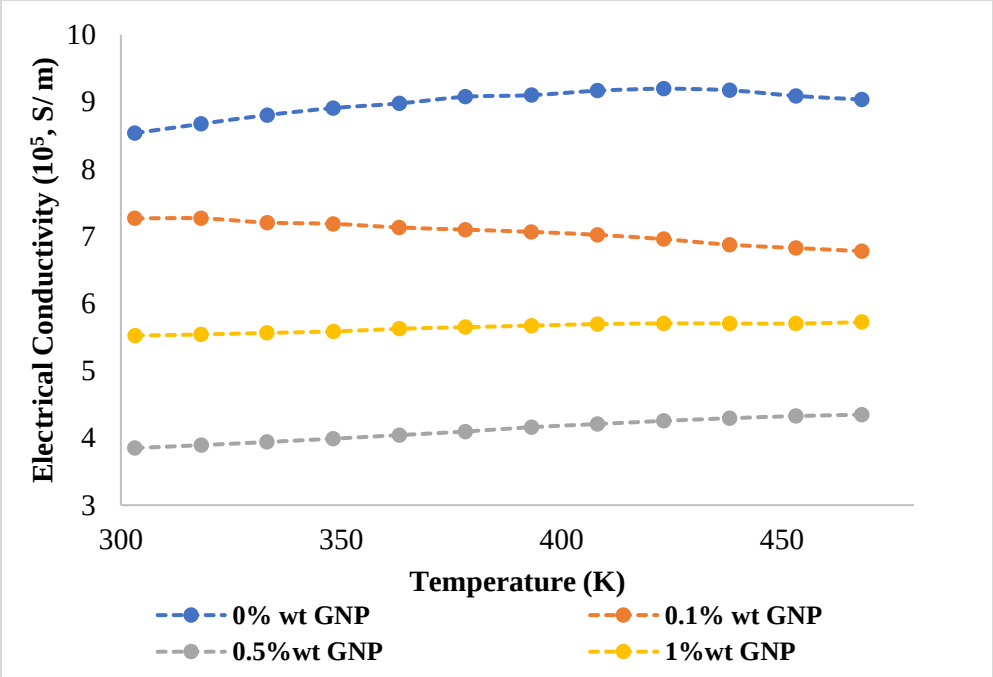

Figure 30. Electrical conductivity (10^5, S/m) for composite material bulk p-type BiTe with 0, 0.1, 0.5 and 1% wt GNP.

Figure 31, shows the thermal conductivity for composite material bulk p-type BiTe with 0, 0.1, 0.5 and 1% wt GNP, it is also observed that when increasing the percentage of graphite nanoplatelets the conductivity between the samples decreases, the sample bulk p-type BiTe with 0.5%wt GNP presented the lowest conductivity. Independent analysis of the samples shows an upward tendency of thermal conductivity to increase temperature.

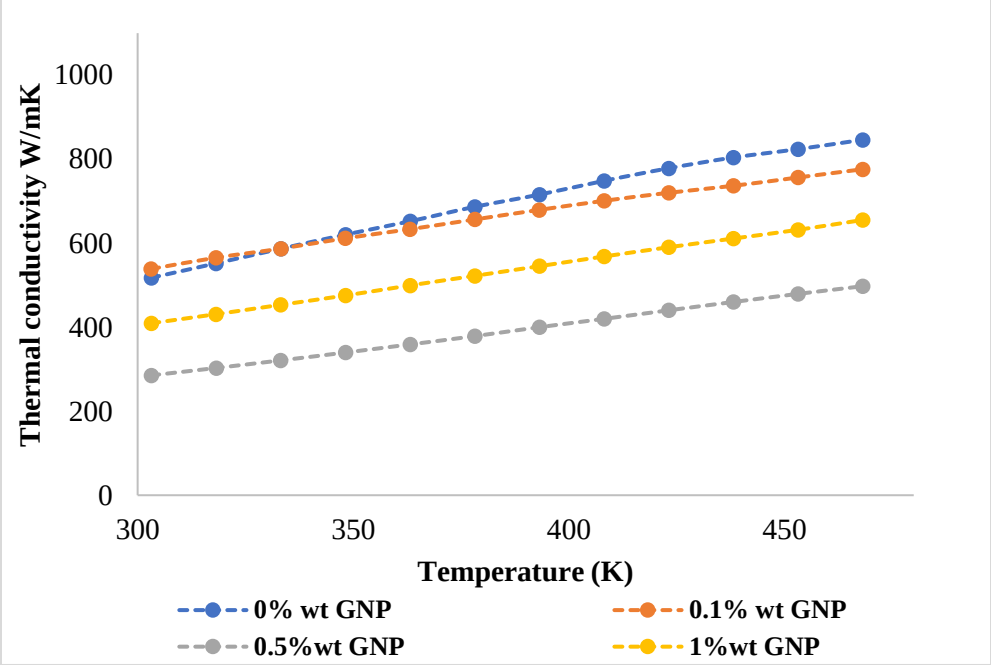

Figure 31. Thermal conductivity (W/mK) for composite material bulk p-type BiTe with 0, 0.1, 0.5 and 1% wt GNP.

The values of the Hall coefficient have a fluctuating behavior (see Figure 32), but it is evident that in all samples the Hall coefficient tends to decrease with the increase in temperature, its positive value indicates that the predominant carriers in the sample are holes typical of p-type semiconductors. The 0%wt GNP sample is the one that presents a more notable variation in the Hall coefficient and in the SEM-EDS analysis it was also the sample that presented the highest percentage of oxygen (see **Table 10**)

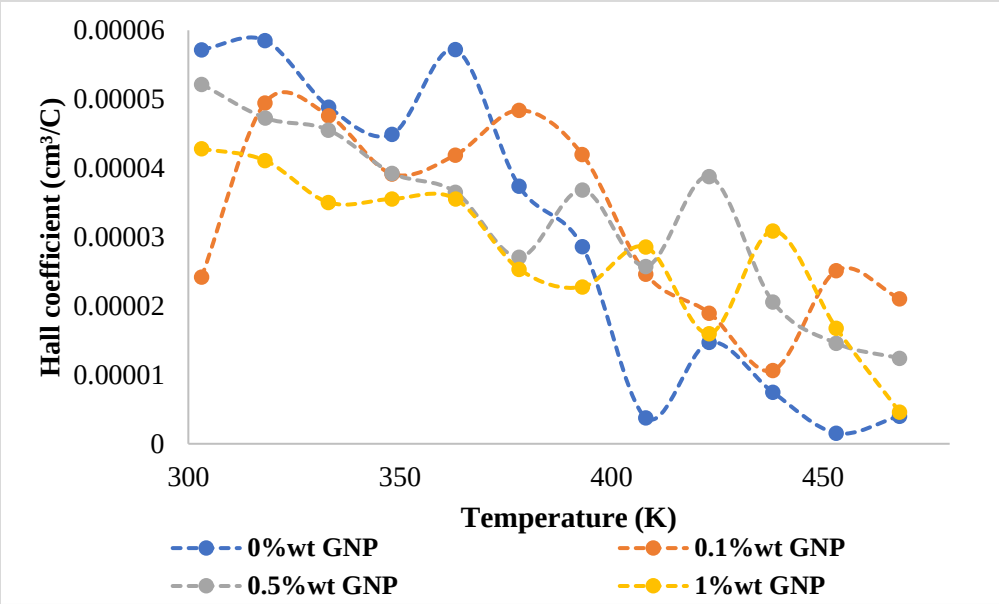

Figure 32. Hall Coefficient (cm³/°C) for composite material bulk p-type BiTe with 0, 0.1, 0.5 and 1% wt GNP.

The mobility of carriers also presents a fluctuating behavior in all more samples and this property tends to decrease with increasing temperature in the samples, samples with 0%wt GNP and 0.1%wt GNP are those that present a more notable change in this property.

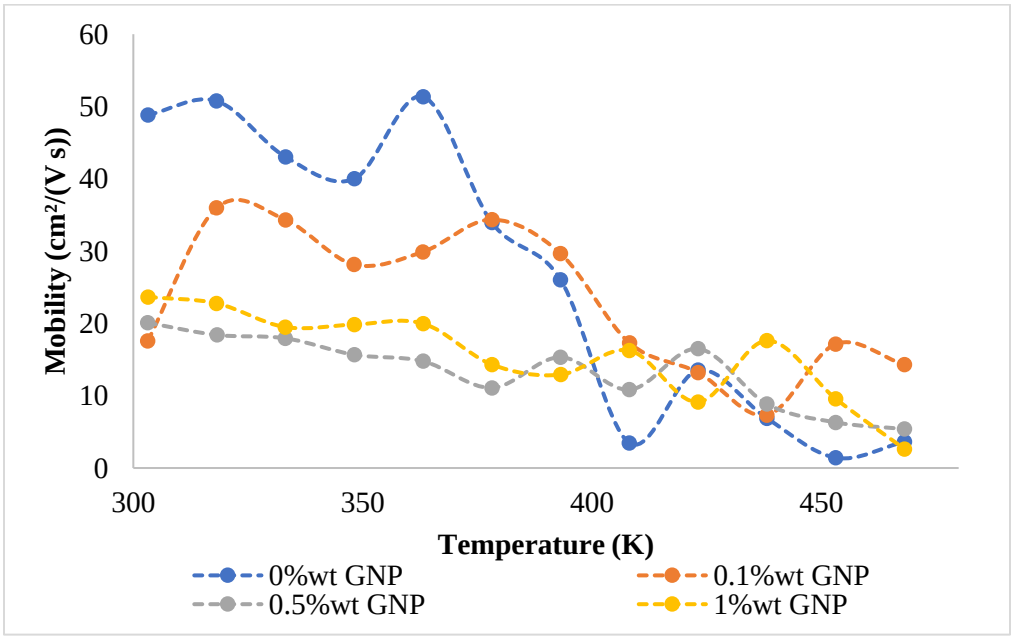

Figure 33. Movility (cm/(Vs) for composite material bulk p-type BiTe with 0, 0.1, 0.5 and 1% wt GNP.

The positive values of the Seebeck coefficient (see Figure 34) indicate that the majority charge carriers in the material are hollow, characteristic of p-type semiconductors. It is observed that when increasing the percentage of nanoplatelets in the material the Sebeeck coefficient decreases, samples with 0 and 0.5% wt GNP presents a similar Seebeck coefficient, the sample 1%wt GNP was the one that presents a lower Seebeck coefficient.

When comparing the seebeck coefficient of manufactured composite materials and those found in the literature, an improvement can be identified since in many cases the Seebeck coefficient does not exceed 200 μV/K [17], [118]–[122] and for samples with 0 and 0.1%wt GNP values of up to 250 μV/K were obtained.

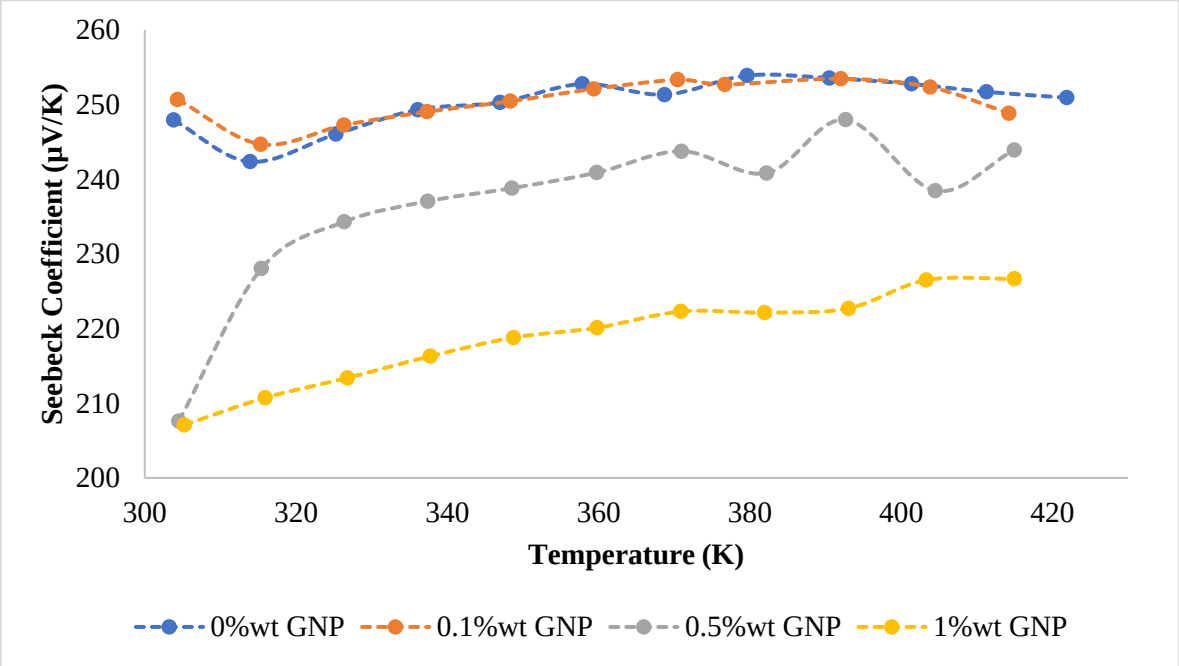

Figure 34. Seebeck coefficient (μV/K) for composite material bulk p-type BiTe with 0, 0.1, 0.5, and 1% wt GNP.

To improve the thermoelectric capacity of a material, what is expected is to be able to increase its capacity to conduct electricity (electrons or electron holes) and decrease its thermal conductivity (phonon dispersion) in the presence of temperature, in this case, the bulk composite material p-type BiTe with 0, 0.1, 0.5 and 1% wt GNP present an opposite behavior since the electrical conductivity of the material decreases with temperature, and thermal conductivity increases with temperature; additionally, fluctuations in mobility measures, Hall coefficient, and Seebeck coefficient are undesirable characteristics in a thermoelectric material.

The behavior in the thermoelectric properties of manufactured composite materials can be attributed to many factors, such as variation in particle size and oxidation[114], [123], [124], which is one of the factors that most harm the manufacture of this type of material. As observed, all samples presented a percentage of oxygen that was detected in the SEM/EDS analysis.

Therefore, it is recommended to have the entire manufacturing process controlled with a controlled atmosphere and perform complementary characterization tests such as Raman spectroscopy or transmission electron microscopy (TEM) during each stage of the manufacturing process to verify the timely detection of oxygen present in the samples and avoid the influence of this on the final properties of the material.

5.1. Conclusions

- The addition of graphite nanoplatelets does not generate an evident improvement in the thermoelectric properties of the material, if it is observed that the values obtained of electrical conductivity, thermal conductivity and Seebeck coefficient after the manufacturing process of ball grinding with controlled atmosphere, cold pressed and vacuum sintering when increasing the content of nanoplatelets generated a decrease in properties. Despite this, the materials manufactured are outstanding with respect to the values reported in the literature. Materials with 0% and 0.1%wt GNP exhibited better performance in thermoelectric properties.
- The particle size of the material, defects and impurities also directly affect the behavior of the carriers, as observed in the results of the thermoelectric properties, the Hall coefficient and mobility had a highly fluctuating behavior.

- The oxygen content in manufactured composite materials can be a relevant factor because it can influence the behavior of the carriers which directly affects the thermoelectric properties.

- An in-depth study of the use of stearic acid ($C_{18}H_{36}O_2$) as a process controller agent (PCA) used to avoid agglomerations of the material in the ball grinding process should be carried out, because this can interfere with the percentage of carbon in the material as observed in the SEM/EDS tests for the p-type BiTe material with 0% wt GNP which presented an unusual carbon percentage since this particular sample had no graphite nanoplatelets, but had 2% GWP.

CHAPTER 6

Chapter published: "Thermoelectric Generator Using Low-Cost Thermoelectric Modules for Low-Temperature Waste Heat Recovery" **Published in Sustainability magazine in February 2023. DOI: https://doi.org/10.3390/su15043681**

6. Thermoelectric generator system (TGS)

In this study, two low-cost thermoelectric modules were characterized, a refrigeration module reference TEC1-12706 (TEC) and a thermoelectric generation module reference SP1848-27145SA (SP), with the aim of manufacturing a thermoelectric generator system (TGS) for the recovery of waste heat at a low-medium temperature at an industrial level. The modules were evaluated at the laboratory level in different configurations, distances from the source, and with a finned heat dissipation system to establish improved energy recovery conditions. The manufactured TGS was designed for heat recovery in low-medium residual temperature processes and was tested in an industrial drying oven of the Sumicol SAS company.

This section provides an overview of the efficiency and challenges of incorporating thermoelectric heat recovery systems made with economic thermoelectric cells marketed in Latin America when evaluated at the laboratory level (under controlled conditions) and at an industrial level (under uncontrollable conditions). The project is part of a local strategy to improve materials circularity [125], [126] and energy optimization [127]–[129] in materials and industrial processes in the country, issues relegated to importance for decades at the legislative and technological level. The case study presented here is applicable elsewhere and is particularly an inexpensive and green solution feasible to run in developing countries where generation cells are difficult to obtain.

6.1. Materials and Methodology

6.1.1. Materials

The structural assembly of the TGS was designed, which included two complementary components: a metal plate that might need to be in contact with the brink of the warmth source and a finned conductor component for cooling the cold face of the modules, aiming to improve the temperature difference on the faces of the thermoelectric modules. Subsequently, between the metal conductor, and the thermoelectric modules were placed, see Figure 35.

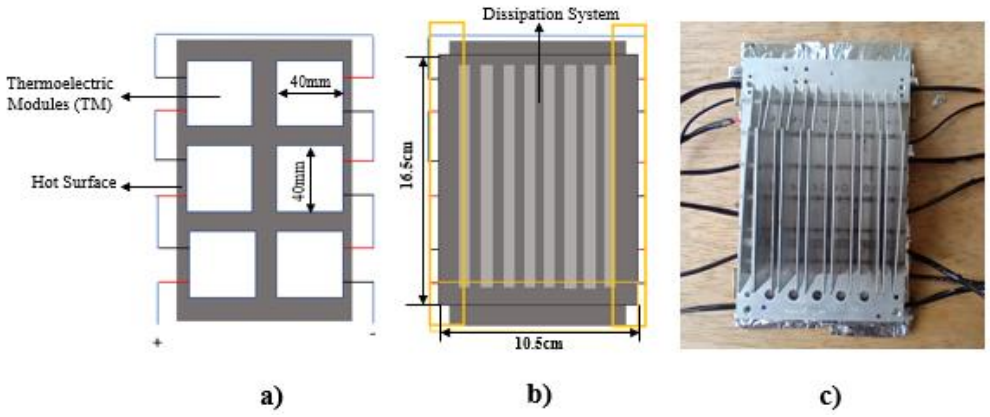

Figure 35. Mounting design of the TGS of 6 modules n. a) Electrical interconnection of the TGS of 6 modules; b) Schematic configuration; c) Actual assembly.

Table 11 shows the technical specifications of the thermoelectric modules **SP1848-27145SA (TEG-GEN) and TEC1-12706 (TEC-REF)** used to assemble the TGS.

Table 11. Technical specifications of the references of the thermoelectric modules [130]

SP1848-27145SA (TEG-GEN)		**TEC1-12706 (TEC-REF)**	
Cost ($US)	3.50	**Cost ($US)**	3.05
Dimensions(mm)	40 x 40 x 3.4	**Dimensions (mm)**	40x40x3.8
Maximum temperature difference (°C)	100	**Max. temp. difference between faces (°C)**	66-75
Nominal current (mA)	669	**Maximum current (A)**	6.4
Maximum open circuit voltage (V)	4.8	**Maximum Voltage (V)**	16.4
Nominal power (W)	------	**Nominal power (W)**	72
Hot side temperature (°C)	150	**Hot side temperature (°C)**	50-57
Thermal conductivity (W/cm.° C)	1.6	**Thermal conductivity (W/cm.° C)**	1.2

6.1.2. Methodology

An assembly was implemented in which the heat was supplied through electrical resistances, from which the voltage (mV) and current (mA) values recorded by different TGS configurations were measured. The TGS configurations were made up of arrangements of 2 and 6 interconnected thermoelectric modules. In the case of the TGS made up of 2 thermoelectric modules, serial and parallel connections were implemented, while for the TGS made up of 6 thermoelectric modules, serial and mixed connections (combination between modules connected in series and in parallel, see Figure 3) were employed. Likewise, two distances from the TGS to the heat source were evaluated.

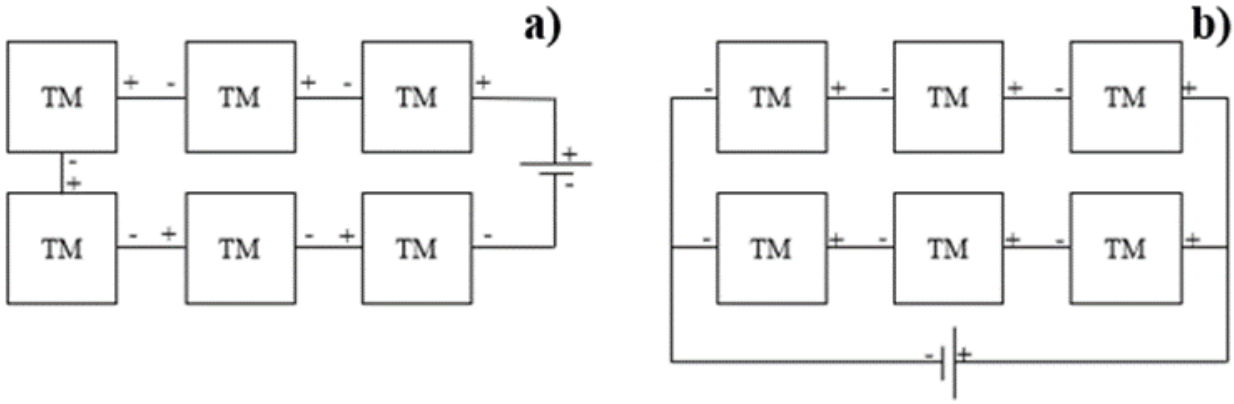

Figure 36. Outline of the TGS made up of 6 thermoelectric modules in a) serial connection and b) mixed connection.

Finally, an in-situ large-scale company installation was implemented using the assembly of the TGS made up of 6 modules, with the same connections used at the laboratory level, but now with a real process going on (Figure 37). The heat source, in this case, was the surface of a drying oven of the Colombian company Sumicol SAS, the larger scale company of traditional ceramics in Colombia. In this process, a measurement of the surface temperature of the furnace wall was made using thermographic techniques. The TGS was mounted vertically, and the respective Voltage (mV) and current (mA) measurements were made.

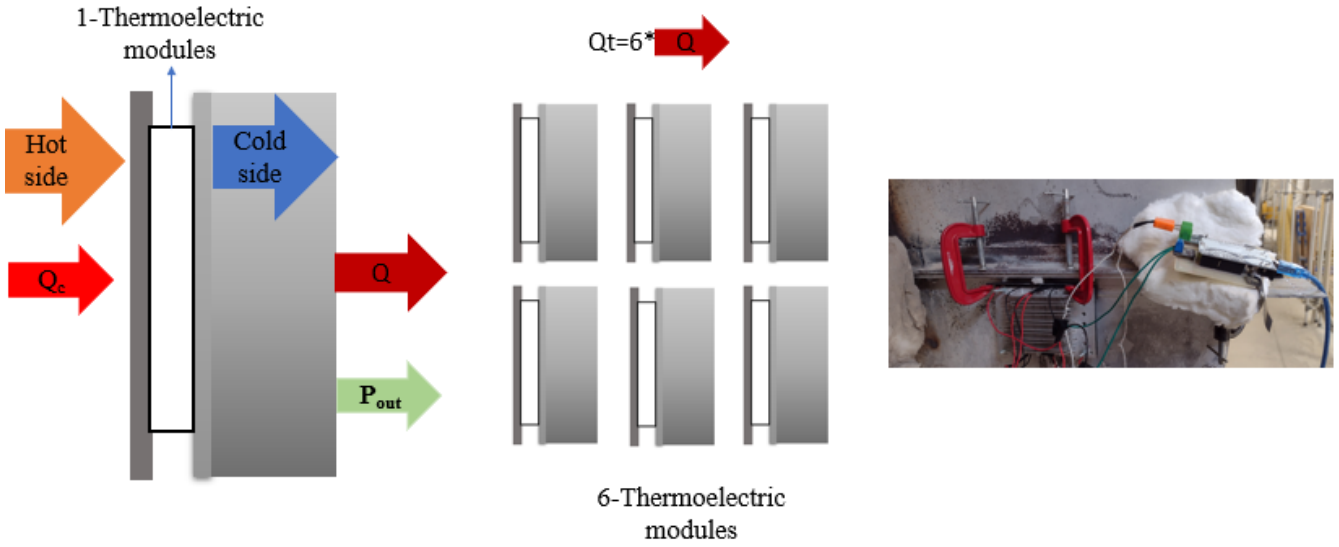

Figure 37. Basic diagram for the power generation of the TGS made up of 6 thermoelectric modules.

In Figure 38, Diagram of the assembly of the experimental platform consisting of the thermoelectric generator with the cells and the fin-type dissipation system, the data acquisition system which delivers the information of cold side temperature, hot side temperature, temperature delta (temperature range: 0 to 800 ° C), voltage (range: 0V to 26 V DC) and current (range: 0 to 3.2A) in Microsoft Excel.

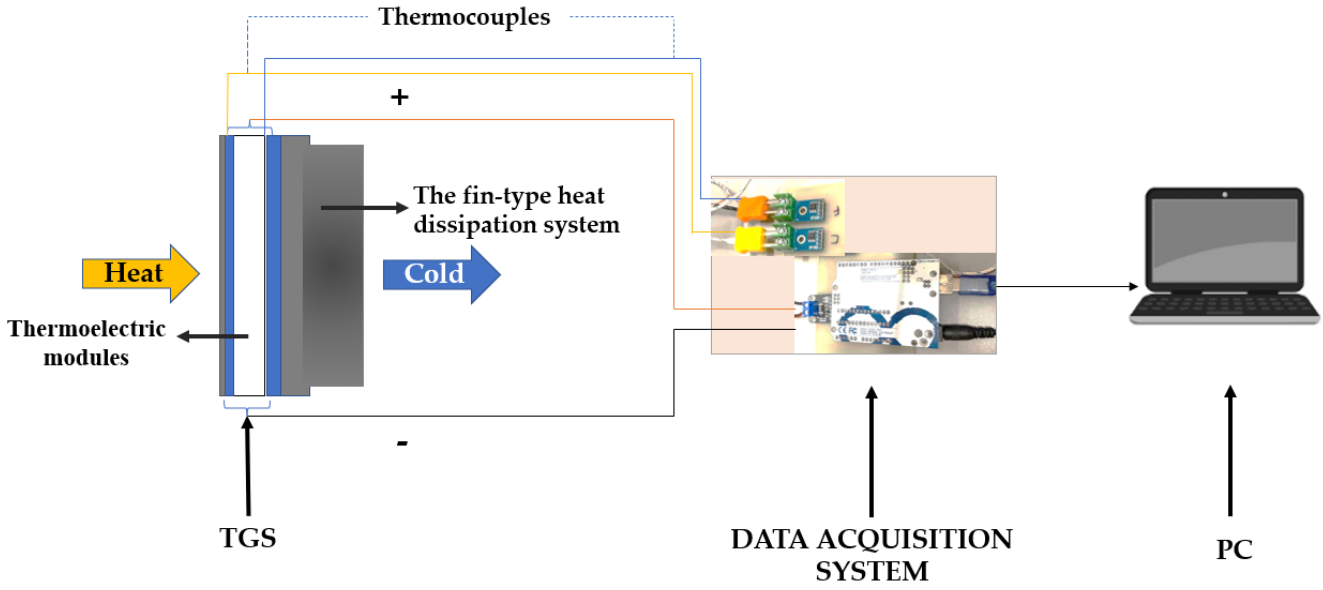

Figure 38. Diagram of the assembly of the experimental platform

6.2. Results and discussion

The modules used (see Table 11) do not present a significant difference in their cost, the SP1848-27145SA module being $0.45 US more expensive than the TEC1-12706 module. The technical sheet of the two types of modules is quite different due to the targeted application for which each one is commercially directed. The SP1848-27145SA module is sold as a generation module capable of withstanding a maximum temperature of 100°C between faces, and the TEC1-12706 module is sold as a cooling module and supports a temperature range of 66-75°C between faces. The modules evaluated are composed of bismuth telluride-based materials, both n-type and p-type.

The evaluation of different TGSs was carried out under the experiment design shown in Table 12, which specifies the parameters for both laboratory and industrial-level tests in the drying oven.

Table 12. Design of experiments for the thermoelectric generator at the laboratory and industrial levels.

TGS Designation	Leves test	Module type	# Modules	Connection type	Distance from source
2TEG-GEN-S-10cm	Laboratory	TEG-GEN	2	Serial	10 cm
2TEG-GEN-P-5cm	Laboratory	TEG-GEN	2	Parallel	5 cm
2TEC-REF-S-10cm	Laboratory	TEC-REF	2	Serial	10 cm
2TEC-REF-S-5cm	Laboratory	TEC-REF	2	Parallel	5 cm
6TEG-GEN-S-2cm	Laboratory	TEG-GEN	6	Serial	2cm
6TEG-GEN-M-2cm	Laboratory	TEG-GEN	6	Mixed	2cm
6TEG-REF-S-2cm	Laboratory	TEC-REF	6	Serial	2cm
6TEG-REF-M-2cm	Laboratory	TEC-REF	6	Mixed	2cm
6TEG-GEN-S-5cm	Industry	TEG-GEN	6	Serial	5cm
6TEG-GEN-M-5cm	Industry	TEG-GEN	6	Mixed	5cm
6TEG-REF-S-5cm	Industry	TEC-REF	6	Serial	5cm
6TEG-REF-M-5cm	Industry	TEC-REF	6	Mixed	5cm

6.2.1. Characterization of commercial thermoelectric cells and construction of the TGS

In Figure 39, the results of the laboratory tests for two TGS of each reference are shown. The modules used were SP1848-2714SA (TEG GEN) and TEC-12706 (TEC REF) in series and parallel connections at different distances (5 and 10 cm from the heat source). The average temperature of the source was 530 ±3 °C.

For the two cell references, a higher power generation could be observed when the connection between the modules is in parallel. In the case of the reference SP1848-2714SA, the configuration that exhibited the better Voltage and current recovery was obtained through parallel connections with a distance of 5cm from the source that reached a temperature difference of 22.25 °C (Tc = 70.75 °C and Th = 93 °C) and obtained a voltage of 1068 mV and a current of 106.1 mA. In this configuration, despite presenting the best performance when reaching maximum difference temperature for each case, the current and Voltage began to decrease.

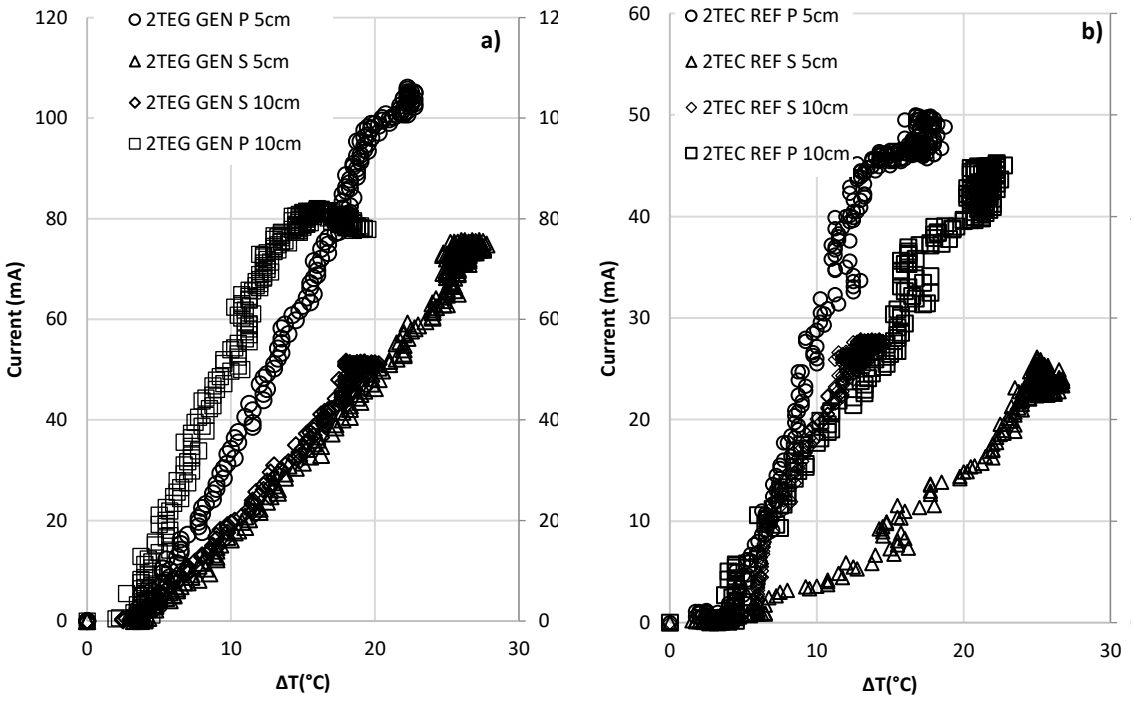

Figure 39. Results of electrical power vs. differential temperature for laboratory TGS tests of two thermoelectric modules a) TEG- SP1848-2714SA; b) TEC-12706.

The reference of modules TEC-12706 presented a better performance in the configuration parallel to 5cm of distance from the source at a different temperature of 17.5 °C (Tc = 78.75 °C and Th = 96.25 °C) obtained a voltage of 506.4 mV and a current of 49.8 mA. It can be seen in Table 13 that not only

is a large difference in temperature between the faces of the cells important since this does not guarantee a good performance in the generation of power as can be seen in the tests 2TEC REF P 5CM and 2TEC REF S 5cm in which the difference temperature is not directly linked to the Voltage, current or electrical power generated by the cells.

Table 13. Results of the maximum energy recovery values in laboratory tests on two thermoelectric cells at the laboratory level.

TGS	T. Cold (Tc) (°C)	T. Hot (Th) (°C)	Difference Temp (°K)	Electrical Voltage (mV)	Electrical Current (mA)	Electrical Power (W)	$\%E_R$
2TEG GEN P 5CM	70.75	93.00	22.25	1068.00	106.10	113.31	3.38
2TEG GEN S 5CM	69.25	96.00	26.75	762.60	75.50	26.78	1.43
2TEG GEN P10CM	64.50	80.50	16.00	820.00	80.80	66.26	2.75
2TEG GEN S 10CM	65.25	84.25	19.00	521.00	51.40	57.58	0.94
2TEC REF P 5CM	78.75	96.25	17.50	506.40	49.80	25.22	1.43
2TEC REF S 5CM	80.5	105.75	25.25	256.00	25.50	20.13	0.26
2TEC REF P 10CM	68.25	90.50	22.25	452.40	44.50	7.56	0.90
2TEC REF S 10CM	75.75	90.00	14.25	279.00	27.10	6.53	0.53

In the TGS GEN P 5cm and 2TEC REF P 10 cm, it was observed that the maximum generation for each of the cells was given for a different temperature of 22.25 °C. This differential temperature is given in very similar values of the cold and hot face of the cells in the two tests, but the voltage generation and electrical power reflect the generation capacity of each of the cells, as can observe that the SP1848-2714SA cells come to generate more than double the energy generated by the TEC-12706 cell under the same conditions, this due to the nature of the modules that in the case of the latter are manufactured for thermoelectric cooling, while sp1848-2714SA cells are generating cells and support a much higher temperature range.

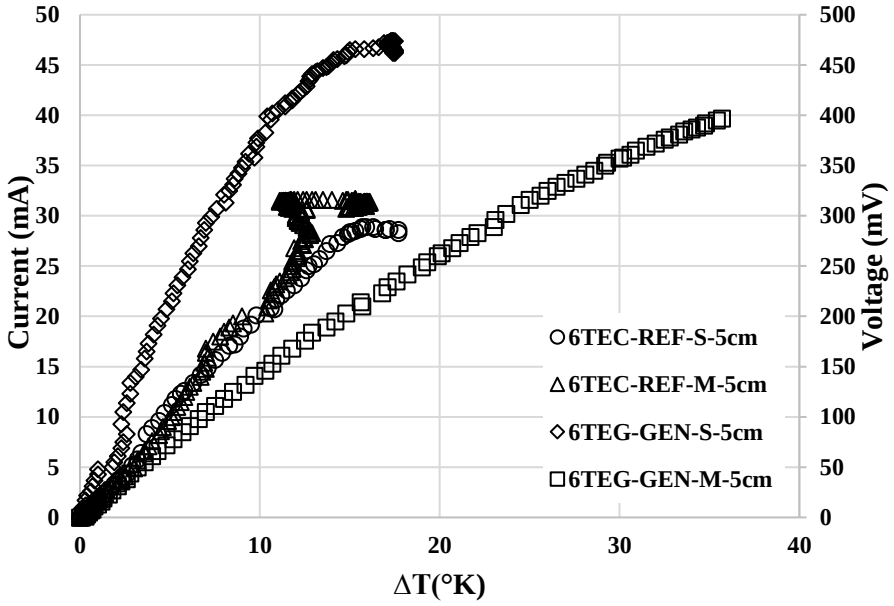

Figure 40. Results of laboratory tests with TGS of 6 thermoelectric cells electric Voltage vs. differential temperature and electric current vs. differential temperature.

Figure 40 shows the voltage and current production for thermoelectric cells for laboratory-level tests for six thermoelectric modules SP1848-2714SA and TEC-12706 in mixed and serial connection. The results obtained for the TEC1-10706 modules in the different connections 6TEC-REF-S-5cm and 6TEC-REF-M-5cm do not show a significant difference in power generation. On the other hand, among the connections in which the SP1848-27145SA modules were evaluated, if a significant difference was observed with respect to the type of connection, for the 6TEG-GEN-M-5cm test in which two groups of 3 modules were connected in series and then connected in parallel, the difference temperature that was reached was 35°C and a power generation of 40mA and 400mV, compared to the 6TEG-GEN-S-5cm test in which the modules were connected in series, the power generation was higher than 47 mA and 450mV, but the maximum difference temperature before the cells began to decrease the current generation was 17 ° C.

Table 14. Results obtained to evaluate heat recovery efficiency in of laboratory tests with TGS of 6 thermoelectric cells.

Test	ΔT (°K)	P_{out} (mW)	Q_T (W)	% E_R
6TEC-REF-M-5cm	16.3	6.74	4941.47	0.17
6TEC-REF-S-5cm	15.3	1.99	4638.32	0.22
6TEG-GEN-M-5cm	17.3	14.71	7815.53	0.29
6TEG-GEN-S-5cm	35.7	4.83	16128.00	0.10

6.2.2. Industrial-level tests in a drying oven of the Sumicol S.A.S company

When characterizing the heat source, in this case, the drying oven of the company Sumicol S.A.S (see Figure 41), it was found that it had an approximate surface temperature of 163 ± 54 °C. Therefore, the assembly was carried out with the configurations of table 2 and the results of the differential temperature between the faces of the cell, electrical Voltage, and electric power generated can be seen in Figure 41.

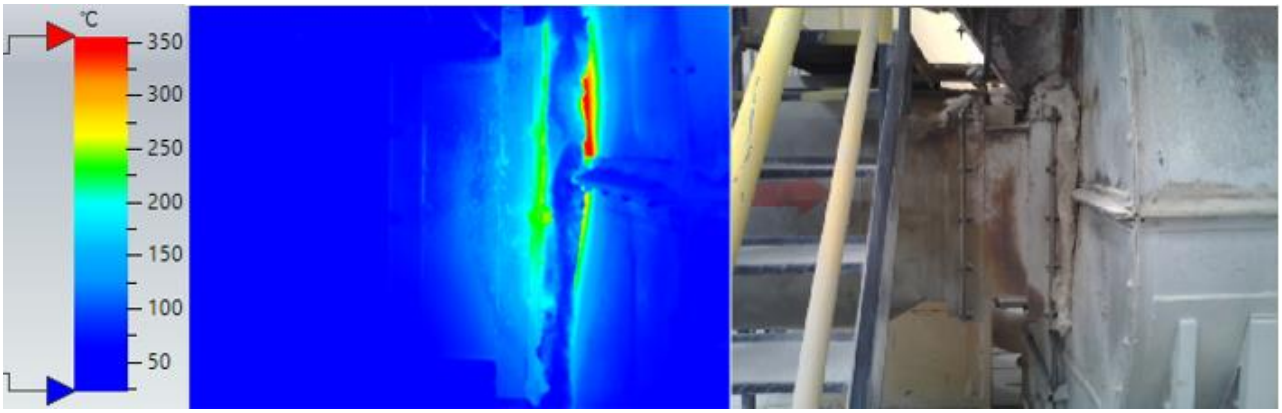

Figure 41. Thermography of the hot surface of the drying oven.

In Figure 42 a), it is observed that the differential of temperature for the different TGS is small, and between test and test, they vary; this is because the parameters of the furnace are constantly modified because the material to be dried can arrive with different humidity. Therefore, the operator in charge makes variations in the operating parameters of the furnace, thus also generating heating of the ambient temperature making the fin-type heat dissipation system not enough to maintain a good difference temperature between the faces of the modules. In Figure 42 b) and c), it can see that the best TGS generation was obtained with the 6TEG-GEN-M-2cm. In general, the mixed connections for the different thermoelectric modules presented better generation than the serial connections. There was also evidence of a fluctuation in the values of the collected data.

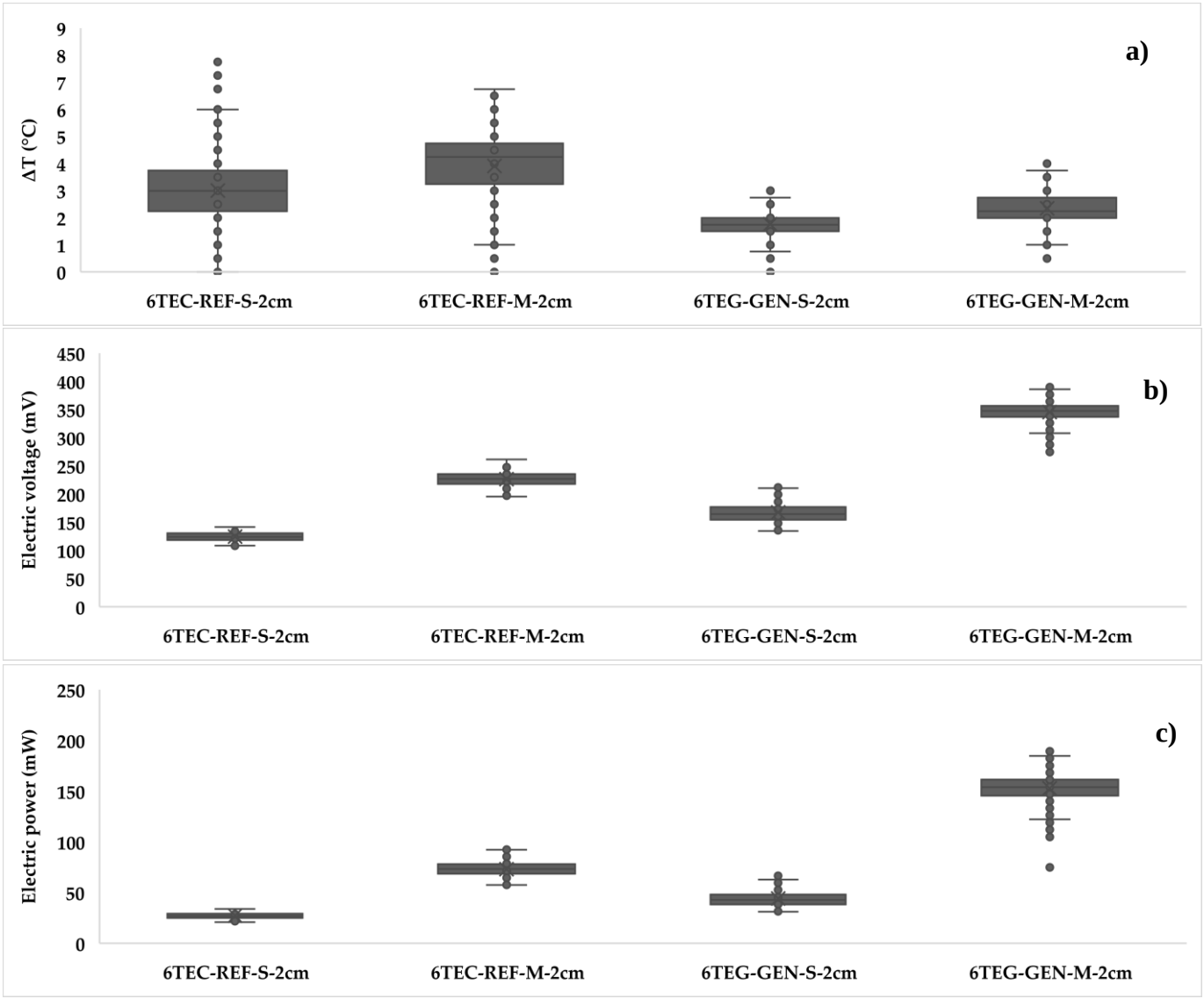

Figure 42. Results of a) difference in temperature between the faces of the cell, b) electrical voltage, c) electrical power.

This was taken as a single system to evaluate the heat recovery efficiency of the manufactured thermoelectric generator, regardless of the number of thermoelectric modules used. First, an energy balance was made, in which the basic energy equations were raised. A steady state is assumed, without resistance to contact, without radiation. There is the conversion by convection on the internal faces of the thermoelectric modules; therefore, the heat flow calculated in the system remains constant and is evaluated by means of the equation:

$$Q = kA\frac{\Delta T}{\Delta x} \qquad (1)$$

Where k is the thermal conductivity of the module, A is the cross-section of the module, and Δx is the thickness of the module. The ΔT used to find the heat for each of the thermoelectric generator configurations was the ΔT corresponding to the highest value of electrical power generated during the experimental part.

Equation (1) is the heat flow for a single cell, as the system evaluated at an industrial level in the drying oven is composed of 6 cells; this value is multiplied by the total number of cells to obtain the total heat flux of the theoretical system in Watt, see equation (2).

$$Q_T = 6 * Q \qquad (2)$$

To find the percentage of electrical power recovered is calculated as follows:

$$\%E_R = \frac{P_{out}}{Q_T} \qquad (3)$$

With Pout, it is the maximum electrical power reached by each configuration. In Table 15 and Figure 43, we can see the results obtained.

Table 15. Results obtained to evaluate heat recovery efficiency.

TEST	ΔT (°K)	P_{OUT} (W)	Q_T (W)	% E_R
6TEC-REF-M-2cm	6	6.74	2273.68	0.30
6TEC-REF-S-2cm	0.75	1.99	284.21	0.70
6TEG-GEN-M-2cm	2.75	14.71	1242.35	1.18
6TEG-GEN-S-2cm	1.5	4.83	677.65	0.71

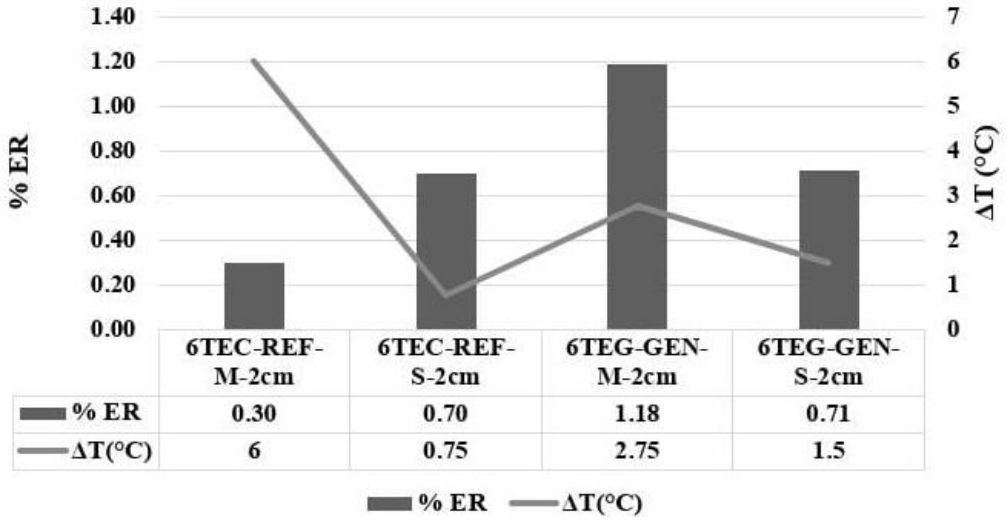

Figure 43. Heat recovery efficiency and ΔT.

It is evident that the maximum heat recovery efficiency was 1.18% for the 6TEG-GEN-M-2cm test, in which the SP 1848-27145 cells of thermoelectric generation in mixed connection were used. This low heat recovery can be attributed to the low difference temperature that was achieved with the finned heatsink because the constant operation of the drying oven generated that the ambient temperature increased preventing temperature deltas from having temperature deltas high between the faces of the cells.

As expected and revealed in Figure 39, with less distance to the head source, more current is recovered (also Voltage and power), which also correspond to a less temperature difference, therefore taking more advantage when compared to cells positioned farther to the head source. When thermoelectric refrigeration cells (TEC-REF) and thermoelectric generation cells (TEG-GEN) are globally compared, see Figure 39, TEG-GEN produced nearly 50% more current than TEC-REF, which justifies their use recommended by the manufacturer.

From the results presented above, it is clear that the thermoelectric refrigeration cells (TEC-REF) are not recommended for a generation due to their low costs and poor availability could be used in many developing countries where regular generation thermoelectric modules are unfeasible. This could be a good alternative for recovering thermal energy and, perhaps upon a process optimization, be used in the industry under controlled conditions, particularly controlling thermal shock, high temperature, and handling. Also, Figure 43 shows the use of 6 cells package, in general, is quite suitable for both systems, besides the fluctuations between the cells and their repeatability.

The configurations of primary connections in series and parallel were made in order to find which connection presented a better performance for the voltage drop that the direct current circuit could have in the generator, throwing at the laboratory level higher voltage values in the series configuration, then for the experimental phase at the industrial level, the mixed configuration was made in order to have a better balance between The Voltage and current generated without having significant effects on the measurements of these parameters by the voltage drop due to external arrangements such as the size of the cables used in the two experimental stages. In this last stage, it is evident that, although the temperature delta is not very high, the configuration that presents better performance is the mixed one.

On the other hand, Latin America and many other areas of the world have a lot of wasted energy from industrial sources released by chimneys poorly or not optimized at all for fewer emissions of gasses, fumes, and heat. Any solution towards the circular economy for particle and gas emission reduction may also consider heat waste reduction, which is not implemented at all in many countries. Therefore, heat recovery must be considered in the equation if sustainable processing is the goal, and thermoelectric is a direct way to recover this.

By observing the results obtained, the implementation of a hybrid heat dissipation system that uses the recirculation of air or wastewater from industrial processes can be a promising alternative for thermoelectric generators to improve their efficiency in an environmentally friendly way using the circular economy.

6.3. Conclusions

- An adequate coupling between the parts of the generation system promotes the best performance of the thermoelectric modules.
- The TEC1-12706 and SP 1848-27145 generation cooling cells are modules for low-temperature applications. In the tests carried out, the temperature of the hot face of the module can reach a maximum temperature of 120 ° C when the assembly is 5 cm from the source, which may explain the fluctuations in the measurements and the mechanical failures in the cells.
- The speed of variation of the temperature gradient is a determining factor in the power value generated by the module system, because the two sides of the cell can reach the same temperature very quickly, decreasing the efficiency of the thermoelectric modules.
- A heat dissipation mechanism that allows the temperature gradient between the cell faces to be maintained for longer promotes the optimal performance of the generation system, guaranteeing higher voltages and better system performance.
- the maximum heat recovery efficiency was 1.18% for the 6TEG-GEN-M-2cm test, in which the SP 1848-27145 cells of thermoelectric generation in mixed connection were used.

Future work

- It is recommended for future work to implement a hybrid heat dissipation system that uses the recirculation of air or wastewater from industrial processes to increase the temperature delta and obtain better performance of the modules.

Appendix

Publications in scientific journals

M. Castañeda, E. I. Gutiérrez-Velásquez, C. E. Aguilar, S. N. Monteiro, A. A. Amell, and H. A. Colorado, “Sustainability and Circular Economy Perspectives of Materials for Thermoelectric Modules,” *Sustainability (Switzerland)*, vol. 14, no. 10. MDPI, May 01, 2022. doi: 10.3390/su14105987.

Participation in scientific events

TMS 2022 150 th Annual Meeting & Exhibition. Conference held from February 27 – March 3, 2022, in Anaheim, California, U.S.A. Role in the event: Speaker " Thermoelectric Generators System Made with Low-Cost Thermoelectric Modules for Low Temperature Waste Heat Recovery. "

References

[1] H. Fang, J. Xia, K. Zhu, Y. Su, and Y. Jiang, "Industrial waste heat utilization for low temperature district heating," *Energy Policy*, vol. 62, pp. 236–246, Nov. 2013, doi: 10.1016/j.enpol.2013.06.104.

[2] A. Firth, B. Zhang, and A. Yang, "Quantification of global waste heat and its environmental effects," *Appl Energy*, vol. 235, no. November 2018, pp. 1314–1334, Feb. 2019, doi: 10.1016/j.apenergy.2018.10.102.

[3] C. Forman, I. K. Muritala, R. Pardemann, and B. Meyer, "Estimating the global waste heat potential," *Renewable and Sustainable Energy Reviews*, vol. 57, pp. 1568–1579, May 2016, doi: 10.1016/j.rser.2015.12.192.

[4] H. Jouhara and A. G. Olabi, "Editorial: Industrial waste heat recovery," *Energy*, vol. 160, pp. 1–2, Oct. 2018, doi: 10.1016/j.energy.2018.07.013.

[5] M. Papapetrou, G. Kosmadakis, A. Cipollina, U. la Commare, and G. Micale, "Industrial waste heat: Estimation of the technically available resource in the EU per industrial sector, temperature level and country," *Appl Therm Eng*, vol. 138, pp. 207–216, Jun. 2018, doi: 10.1016/j.applthermaleng.2018.04.043.

[6] E. Woolley, Y. Luo, and A. Simeone, "Industrial waste heat recovery: A systematic approach," *Sustainable Energy Technologies and Assessments*, vol. 29, pp. 50–59, Oct. 2018, doi: 10.1016/j.seta.2018.07.001.

[7] Q. Luo *et al.*, "A Thermoelectric Waste-Heat-Recovery System for Portland Cement Rotary Kilns," *J Electron Mater*, vol. 44, no. 6, pp. 1750–1762, Jun. 2015, doi: 10.1007/s11664-014-3543-1.

[8] L. A. Medrano Parra, "Diseño, construccion y evalucion de un generador termoelectrico acoplado a una estufa ecologica," UNIVERSIDAD DE CIENCIAS Y ARTES DE CHIAPAS, 2016.

[9] M. Hong, Z. G. Chen, and J. Zou, "Fundamental and progress of Bi2Te3-based thermoelectric materials," *Chinese Physics B*, vol. 27, no. 4, 2018, doi: 10.1088/1674-1056/27/4/048403.

[10] H. Goldsmid, "Bismuth Telluride and Its Alloys as Materials for Thermoelectric Generation," *Materials*, vol. 7, no. 4, pp. 2577–2592, Mar. 2014, doi: 10.3390/ma7042577.

[11] L. Hu *et al.*, "Tuning Multiscale Microstructures to Enhance Thermoelectric Performance of n-Type Bismuth-Telluride-Based Solid Solutions," *Adv Energy Mater*, vol. 5, no. 17, pp. 1–13, 2015, doi: 10.1002/aenm.201500411.

[12] H. Mamur, M. R. A. Bhuiyan, F. Korkmaz, and M. Nil, "A review on bismuth telluride (Bi 2 Te 3) nanostructure for thermoelectric applications," *Renewable and Sustainable Energy Reviews*, vol. 82, no. July 2016, pp. 4159–4169, 2018, doi: 10.1016/j.rser.2017.10.112.

[13] F. Li, R. Zhai, Y. Wu, Z. Xu, X. Zhao, and T. Zhu, "Enhanced thermoelectric performance of n-type bismuth-telluride-based alloys via In alloying and hot deformation for mid-temperature power generation," *Journal of Materiomics*, vol. 4, no. 3, pp. 208–214, 2018, doi: 10.1016/j.jmat.2018.05.008.

[14] X. Chen, L. Liu, Y. Dong, L. Wang, L. Chen, and W. Jiang, "Preparation of nano-sized Bi2Te3 thermoelectric material powders by cryogenic grinding," *Progress in Natural Science: Materials International*, vol. 22, no. 3, pp. 201–206, Jun. 2012, doi: 10.1016/j.pnsc.2012.04.006.

[15] G. Delaizir *et al.*, "A comparative study of Spark Plasma Sintering (SPS), Hot Isostatic Pressing (HIP) and microwaves sintering techniques on p-type Bi 2Te 3 thermoelectric properties," *Mater Res Bull*, vol. 47, no. 8, pp. 1954–1960, 2012, doi: 10.1016/j.materresbull.2012.04.019.

[16] S.-J. Jung *et al.*, "Impurity-free, mechanical doping for the reproducible fabrication of the reliable n-type Bi2Te3-based thermoelectric alloys," *Acta Mater*, vol. 150, pp. 153–160, May 2018, doi: 10.1016/j.actamat.2018.02.061.

[17] K. T. Kim, T. S. Min, S. D. Kim, E. A. Choi, D. W. Kim, and S. Y. Choi, "Strain-mediated point defects in thermoelectric p-type bismuth telluride polycrystalline," *Nano Energy*, vol. 55, no. August 2018, pp. 486–493, 2019, doi: 10.1016/j.nanoen.2018.10.069.

[18] J. Yang, R. Chen, X. Fan, S. Bao, and W. Zhu, "Thermoelectric properties of silver-doped n-type Bi2Te 3-based material prepared by mechanical alloying and subsequent hot pressing," *J Alloys Compd*, vol. 407, no. 1–2, pp. 330–333, 2006, doi: 10.1016/j.jallcom.2005.06.041.

[19] K. Ahmad, C. Wan, M. A. Al-Eshaikh, and A. N. Kadachi, "Enhanced thermoelectric performance of Bi 2 Te 3 based graphene nanocomposites," *Appl Surf Sci*, vol. 474, no. November 2017, pp. 2–8, 2019, doi: 10.1016/j.apsusc.2018.10.163.

[20] P. Jagadish *et al.*, "Recycled carbon fibre/Bi2Te3 and Bi2S3 hybrid composite doped with MWCNTs for thermoelectric applications," *Compos B Eng*, vol. 175, no. 5, p. 107085, 2019, doi: 10.1016/j.compositesb.2019.107085.

[21] H. Ju, M. Kim, and J. Kim, "Preparation of graphene sheets into one-dimensionally nanostructured bulk bismuth telluride for enhancing thermoelectric power factor," *Journal of Materials Science: Materials in Electronics*, vol. 27, no. 4, pp. 3427–3434, Apr. 2016, doi: 10.1007/s10854-015-4175-9.

[22] A. H. Li *et al.*, "Electronic structure and thermoelectric properties of Bi2Te3 crystals and graphene-doped Bi2Te3," *Thin Solid Films*, vol. 518, no. 24, pp. e57–e60, Oct. 2010, doi: 10.1016/j.tsf.2010.03.124.

[23] L. D. Zhao, B. P. Zhang, W. S. Liu, H. L. Zhang, and J. F. Li, "Effects of annealing on electrical properties of n-type Bi2Te3 fabricated by mechanical alloying and spark plasma sintering," *J Alloys Compd*, vol. 467, no. 1–2, pp. 91–97, Jan. 2009, doi: 10.1016/j.jallcom.2007.12.063.

[24] K. Agarwal, V. Kaushik, D. Varandani, A. Dhar, and B. R. Mehta, "Nanoscale thermoelectric properties of Bi2Te3 - Graphene nanocomposites: Conducting atomic force, scanning thermal and kelvin probe microscopy studies," *J Alloys Compd*, vol. 681, pp. 394–401, Oct. 2016, doi: 10.1016/j.jallcom.2016.04.161.

[25] M. A. H. El-Meniawi and E. Gewfiel, "Wear Behavior of Graphite Nano Plates/Al Composites," *Physics of Metals and Metallography*, vol. 120, no. 1, pp. 78–86, 2019, doi: 10.1134/S0031918X1808001X.

[26] F. Farooq *et al.*, "A comparative study on performance evaluation of hybrid GNPs/CNTs in conventional and self-compacting mortar," *Alexandria Engineering Journal*, vol. 59, no. 1, pp. 369–379, 2020, doi: 10.1016/j.aej.2019.12.048.

[27] S. Mohammadi, H. Shariatpanahi, F. A. Taromi, and J. Neshati, "Electrochemical and anticorrosion behaviors of hybrid functionalized graphite nano-platelets/tripolyphosphate in epoxy-coated carbon steel," *Mater Res Bull*, vol. 80, pp. 7–22, 2016, doi: 10.1016/j.materresbull.2015.06.052.

[28] S. Chandrasekaran, C. Seidel, and K. Schulte, "Preparation and characterization of graphite nano-platelet (GNP)/epoxy nano-composite: Mechanical, electrical and thermal properties," *Eur Polym J*, vol. 49, no. 12, pp. 3878–3888, Dec. 2013, doi: 10.1016/j.eurpolymj.2013.10.008.

[29] M. Castañeda, E. I. Gutiérrez-Velásquez, C. E. Aguilar, S. N. Monteiro, A. A. Amell, and H. A. Colorado, "Sustainability and Circular Economy Perspectives of Materials for Thermoelectric Modules," *Sustainability (Switzerland)*, vol. 14, no. 10. MDPI, May 01, 2022. doi: 10.3390/su14105987.

[30] B. Jiang *et al.*, "Realizing high-efficiency power generation in low-cost PbS-based thermoelectric materials," *Energy Environ Sci*, vol. 13, no. 2, pp. 579–591, 2020, doi: 10.1039/C9EE03410B.

[31] M. Elzalik, H. Rezk, R. Mostafa, J. Thomas, and E. G. Shehata, "An experimental investigation on electrical performance and characterization of thermoelectric generator," *Int J Energy Res*, vol. 44, no. 1, pp. 128–143, 2020, doi: 10.1002/er.4873.

[32] S. Khanmohammadi, M. Saadat-Targhi, F. W. Ahmed, and M. Afrand, "Potential of thermoelectric waste heat recovery in a combined geothermal, fuel cell and organic Rankine flash cycle (thermodynamic and economic evaluation)," *Int J Hydrogen Energy*, vol. 45, no. 11, pp. 6934–6948, Feb. 2020, doi: 10.1016/j.ijhydene.2019.12.113.

[33] L. Heber and J. Schwab, “Modelling of a thermoelectric generator for heavy-duty natural gas vehicles: Techno-economic approach and experimental investigation,” *Appl Therm Eng*, vol. 174, no. March, p. 115156, Jun. 2020, doi: 10.1016/j.applthermaleng.2020.115156.

[34] P. Halli, B. P. Wilson, T. Hailemariam, P. Latostenmaa, K. Yliniemi, and M. Lundström, “Electrochemical recovery of tellurium from metallurgical industrial waste,” *J Appl Electrochem*, vol. 50, no. 1, pp. 1–14, Jan. 2020, doi: 10.1007/s10800-019-01363-6.

[35] A. Żelazna and J. Gołębiowska, “A PV-Powered TE Cooling System with Heat Recovery: Energy Balance and Environmental Impact Indicators,” *Energies (Basel)*, vol. 13, no. 7, p. 1701, Apr. 2020, doi: 10.3390/en13071701.

[36] O. Velázquez-Martinez *et al.*, “A recycling process for thermoelectric devices developed with the support of statistical entropy analysis,” *Resour Conserv Recycl*, vol. 159, no. December 2019, p. 104843, Aug. 2020, doi: 10.1016/j.resconrec.2020.104843.

[37] T. Ozturk, E. Kilinc, F. Uysal, E. Celik, and H. Kurt, “Effects of Electrical Properties on Determining Materials for Power Generation Enhancement in TEG Modules,” *J Electron Mater*, vol. 48, no. 9, pp. 5409–5417, Sep. 2019, doi: 10.1007/s11664-019-07386-1.

[38] J. Dongxu, W. Zhongbao, J. Pou, S. Mazzoni, S. Rajoo, and A. Romagnoli, “Geometry optimization of thermoelectric modules: Simulation and experimental study,” *Energy Convers Manag*, vol. 195, no. May, pp. 236–243, Sep. 2019, doi: 10.1016/j.enconman.2019.05.003.

[39] R. Merienne, J. Lynn, E. McSweeney, and S. M. O’Shaughnessy, “Thermal cycling of thermoelectric generators: The effect of heating rate,” *Appl Energy*, vol. 237, no. January, pp. 671–681, Mar. 2019, doi: 10.1016/j.apenergy.2019.01.041.

[40] K. Anderson and N. Brandon, “Techno-economic analysis of thermoelectrics for waste heat recovery,” *Energy Sources, Part B: Economics, Planning, and Policy*, vol. 14, no. 4, pp. 147–157, Apr. 2019, doi: 10.1080/15567249.2019.1632976.

[41] C. Han, G. Tan, T. Varghese, M. G. Kanatzidis, and Y. Zhang, “High-Performance PbTe Thermoelectric Films by Scalable and Low-Cost Printing,” *ACS Energy Lett*, vol. 3, no. 4, pp. 818–822, Apr. 2018, doi: 10.1021/acsenergylett.8b00041.

[42] P. Fernández-Yáñez, A. Gómez, R. García-Contreras, and O. Armas, “Evaluating thermoelectric modules in diesel exhaust systems: potential under urban and extra-urban driving conditions,” *J Clean Prod*, vol. 182, pp. 1070–1079, May 2018, doi: 10.1016/j.jclepro.2018.02.006.

[43] S. Wilbrecht and M. Beitelschmidt, “The Potential of a Cascaded TEG System for Waste Heat Usage in Railway Vehicles,” *J Electron Mater*, vol. 47, no. 6, pp. 3358–3369, Jun. 2018, doi: 10.1007/s11664-018-6094-z.

[44] Z. Ouyang and D. Li, "Design of segmented high-performance thermoelectric generators with cost in consideration," *Appl Energy*, vol. 221, no. December 2017, pp. 112–121, Jul. 2018, doi: 10.1016/j.apenergy.2018.03.106.

[45] M. Balva, S. Legeai, L. Garoux, N. Leclerc, and E. Meux, "Dismantling and chemical characterization of spent Peltier thermoelectric devices for antimony, bismuth and tellurium recovery," *Environ Technol*, vol. 38, no. 7, pp. 791–797, Apr. 2017, doi: 10.1080/09593330.2016.1211748.

[46] B. Swain and K.-J. Lee, "Chemical separation of p- and n-type thermoelectric chips from waste thermoelectric module and valorization through synthesis of Bi 2 Te 3 nanopowder: a sustainable process for synthesis of thermoelectric materials," *Journal of Chemical Technology & Biotechnology*, vol. 92, no. 3, pp. 614–622, Mar. 2017, doi: 10.1002/jctb.5042.

[47] H. Lee, R. Chidambaram Seshadri, S. J. Han, and S. Sampath, "TiO 2−X based thermoelectric generators enabled by additive and layered manufacturing," *Appl Energy*, vol. 192, pp. 24–32, Apr. 2017, doi: 10.1016/j.apenergy.2017.02.001.

[48] G. Skomedal *et al.*, "Design, assembly and characterization of silicide-based thermoelectric modules," *Energy Convers Manag*, vol. 110, pp. 13–21, Feb. 2016, doi: 10.1016/j.enconman.2015.11.068.

[49] F. P. Brito *et al.*, "Analysis of the Effect of Module Thickness Reduction on Thermoelectric Generator Output," *J Electron Mater*, vol. 45, no. 3, pp. 1711–1729, Mar. 2016, doi: 10.1007/s11664-015-4182-x.

[50] M. Mori, M. Matsumoto, and M. Ohtani, "Concept for Improving Cost Effectiveness of Thermoelectric Heat Recovery Systems," *SAE International Journal of Passenger Cars - Mechanical Systems*, vol. 9, no. 1, pp. 2016-01–0233, Apr. 2016, doi: 10.4271/2016-01-0233.

[51] T. J. Hendricks, S. Yee, and S. LeBlanc, "Cost Scaling of a Real-World Exhaust Waste Heat Recovery Thermoelectric Generator: A Deeper Dive," *J Electron Mater*, vol. 45, no. 3, pp. 1751–1761, Mar. 2016, doi: 10.1007/s11664-015-4201-y.

[52] C. Fu *et al.*, "Realizing high figure of merit in heavy-band p-type half-Heusler thermoelectric materials," *Nat Commun*, vol. 6, no. 1, p. 8144, Nov. 2015, doi: 10.1038/ncomms9144.

[53] T. Ming *et al.*, "The Influence of Non-Uniform High Heat Flux on Thermal Stress of Thermoelectric Power Generator," *Energies (Basel)*, vol. 8, no. 11, pp. 12584–12602, Nov. 2015, doi: 10.3390/en81112332.

[54] L. T. Hung, N. Van Nong, S. Linderoth, and N. Pryds, "Segmentation of low-cost high efficiency oxide-based thermoelectric materials," *physica status solidi (a)*, vol. 212, no. 4, pp. 767–774, Apr. 2015, doi: 10.1002/pssa.201431626.

[55] I. Arsie, A. Cricchio, V. Marano, C. Pianese, M. de Cesare, and W. Nesci, "Modeling Analysis of Waste Heat Recovery via Thermo Electric Generators for Fuel Economy Improvement and CO 2 Reduction in Small Diesel Engines," *SAE Int J Passeng Cars Electron Electr Syst*, vol. 7, no. 1, pp. 2014-01–0663, Apr. 2014, doi: 10.4271/2014-01-0663.

[56] H. Wang, R. McCarty, J. R. Salvador, A. Yamamoto, and J. König, "Determination of Thermoelectric Module Efficiency: A Survey," *J Electron Mater*, vol. 43, no. 6, pp. 2274–2286, Jun. 2014, doi: 10.1007/s11664-014-3044-2.

[57] A. Rezania, L. A. Rosendahl, and H. Yin, "Parametric optimization of thermoelectric elements footprint for maximum power generation," *J Power Sources*, vol. 255, pp. 151–156, Jun. 2014, doi: 10.1016/j.jpowsour.2014.01.002.

[58] K.-J. Lee, Y.-H. Jin, and M.-S. Kong, "Synthesis of the Thermoelectric Nanopowder Recovered from the Used Thermoelectric Modules," *J Nanosci Nanotechnol*, vol. 14, no. 10, pp. 7919–7922, Oct. 2014, doi: 10.1166/jnn.2014.9422.

[59] A. Patyk, "Thermoelectric generators for efficiency improvement of power generation by motor generators – Environmental and economic perspectives," *Appl Energy*, vol. 102, pp. 1448–1457, Feb. 2013, doi: 10.1016/j.apenergy.2012.09.007.

[60] J. R. Salvador *et al.*, "Thermal to Electrical Energy Conversion of Skutterudite-Based Thermoelectric Modules," *J Electron Mater*, vol. 42, no. 7, pp. 1389–1399, Jul. 2013, doi: 10.1007/s11664-012-2261-9.

[61] W.-B. Kim, "Investigation of Low-Cost, Simple Recycling Process of Waste Thermoelectric Modules Using Chemical Reduction," *Bull Korean Chem Soc*, vol. 34, no. 7, pp. 2167–2170, Jul. 2013, doi: 10.5012/bkcs.2013.34.7.2167.

[62] K. Yazawa and A. Shakouri, "Cost–Performance Analysis and Optimization of Fuel-Burning Thermoelectric Power Generators," *J Electron Mater*, vol. 42, no. 7, pp. 1946–1950, Jul. 2013, doi: 10.1007/s11664-013-2480-8.

[63] K. Yazawa and A. Shakouri, "Scalable Cost/Performance Analysis for Thermoelectric Waste Heat Recovery Systems," *J Electron Mater*, vol. 41, no. 6, pp. 1845–1850, Jun. 2012, doi: 10.1007/s11664-012-2049-y.

[64] G. Homm and P. J. Klar, "Thermoelectric materials - Compromising between high efficiency and materials abundance," *physica status solidi (RRL) - Rapid Research Letters*, vol. 5, no. 9, pp. 324–331, Sep. 2011, doi: 10.1002/pssr.201105084.

[65] K. Yazawa and A. Shakouri, "Cost-Efficiency Trade-off and the Design of Thermoelectric Power Generators," *Environ Sci Technol*, vol. 45, no. 17, pp. 7548–7553, Sep. 2011, doi: 10.1021/es2005418.

[66] C. Babu and P. Ponnambalam, "The role of thermoelectric generators in the hybrid PV/T systems: A review," *Energy Convers Manag*, vol. 151, no. June, pp. 368–385, 2017, doi: 10.1016/j.enconman.2017.08.060.

[67] W. di Liu, Z. G. Chen, and J. Zou, "Eco-Friendly Higher Manganese Silicide Thermoelectric Materials: Progress and Future Challenges," *Adv Energy Mater*, vol. 8, no. 19, pp. 1–18, 2018, doi: 10.1002/aenm.201800056.

[68] W. di Liu, L. Yang, Z. G. Chen, and J. Zou, "Promising and Eco-Friendly Cu2X-Based Thermoelectric Materials: Progress and Applications," *Advanced Materials*, vol. 32, no. 8, pp. 87–92, 2020, doi: 10.1002/adma.201905703.

[69] J. R. C. Rey, D. T. Pio, and L. A. C. Tarelho, "Biomass direct gasification for electricity generation and natural gas replacement in the lime kilns of the pulp and paper industry: A techno-economic analysis," *Energy*, vol. 237, Dec. 2021, doi: 10.1016/j.energy.2021.121562.

[70] Y. Ouyang, Z. Zhang, D. Li, J. Chen, and G. Zhang, "Emerging Theory, Materials, and Screening Methods: New Opportunities for Promoting Thermoelectric Performance," *Annalen der Physik*, vol. 531, no. 4. Wiley-VCH Verlag, Apr. 01, 2019. doi: 10.1002/andp.201800437.

[71] S. D. Huber, "Topological mechanics," *Nat Phys*, vol. 12, no. 7, pp. 621–623, Jul. 2016, doi: 10.1038/nphys3801.

[72] D. Baldomir and D. Faílde, "On Behind the Physics of the Thermoelectricity of Topological Insulators," *Sci Rep*, vol. 9, no. 1, Dec. 2019, doi: 10.1038/s41598-019-42744-3.

[73] L. Shi, J. Chen, G. Zhang, and B. Li, "Thermoelectric figure of merit in Ga-doped [0001] ZnO nanowires," *Physics Letters, Section A: General, Atomic and Solid State Physics*, vol. 376, no. 8–9, pp. 978–981, Feb. 2012, doi: 10.1016/j.physleta.2011.12.040.

[74] B. Qiu, G. Chen, and Z. Tian, "Effects of Aperiodicity and Roughness on Coherent Heat Conduction in Superlattices," *Nanoscale and Microscale Thermophysical Engineering*, vol. 19, no. 4, pp. 272–278, Oct. 2015, doi: 10.1080/15567265.2015.1102186.

[75] R. Fei, A. Faghaninia, R. Soklaski, J. A. Yan, C. Lo, and L. Yang, "Enhanced thermoelectric efficiency via orthogonal electrical and thermal conductances in phosphorene," *Nano Lett*, vol. 14, no. 11, pp. 6393–6399, Nov. 2014, doi: 10.1021/nl502865s.

[76] R. Roldán, J. A. Silva-Guillén, M. P. López-Sancho, F. Guinea, E. Cappelluti, and P. Ordejón, "Electronic properties of single-layer and multilayer transition metal dichalcogenides MX2 (M = Mo, W and X = S, Se)," *Annalen der Physik*, vol. 526, no. 9–10. Wiley-VCH Verlag, pp. 347–357, Oct. 01, 2014. doi: 10.1002/andp.201400128.

[77] A. Ahmad and Y. Singh, "In-plane behaviour of expanded polystyrene core reinforced concrete sandwich panels," *Constr Build Mater*, vol. 269, Feb. 2021, doi: 10.1016/j.conbuildmat.2020.121804.

[78] S. Wolf, N. Neophytou, and H. Kosina, "Thermal conductivity of silicon nanomeshes: Effects of porosity and roughness," *J Appl Phys*, vol. 115, no. 20, May 2014, doi: 10.1063/1.4879242.

[79] T. Ming *et al.*, "The influence of non-uniform high heat flux on thermal stress of thermoelectric power generator," *Energies (Basel)*, vol. 8, no. 11, pp. 12584–12602, 2015, doi: 10.3390/en81112332.

[80] A. Prieto, U. Knaack, T. Auer, and T. Klein, "COOLFACADE: State-of-the-art review and evaluation of solar cooling technologies on their potential for façade integration," *Renewable and Sustainable Energy Reviews*, vol. 101, no. July 2018, pp. 395–414, 2019, doi: 10.1016/j.rser.2018.11.015.

[81] E. Bellos and C. Tzivanidis, "Energy and financial analysis of a solar driven thermoelectric generator," *J Clean Prod*, vol. 264, Aug. 2020, doi: 10.1016/j.jclepro.2020.121534.

[82] H. Alam and S. Ramakrishna, "A review on the enhancement of figure of merit from bulk to nano-thermoelectric materials," *Nano Energy*, vol. 2, no. 2, pp. 190–212, Mar. 2013, doi: 10.1016/j.nanoen.2012.10.005.

[83] S. Shoeibi, H. Kargarsharifabad, M. Sadi, A. Arabkoohsar, and S. A. A. Mirjalily, "A review on using thermoelectric cooling, heating, and electricity generators in solar energy applications," *Sustainable Energy Technologies and Assessments*, vol. 52, p. 102105, Aug. 2022, doi: 10.1016/j.seta.2022.102105.

[84] X. F. Zheng, C. X. Liu, Y. Y. Yan, and Q. Wang, "A review of thermoelectrics research - Recent developments and potentials for sustainable and renewable energy applications," *Renewable and Sustainable Energy Reviews*, vol. 32. pp. 486–503, Apr. 2014. doi: 10.1016/j.rser.2013.12.053.

[85] P. J. Vergragt, "How Technology Could Contribute to a Sustainable World," *Great Transition Initiative: Towards a New Praxis Paper Series*, pp. 1–26, 2006, [Online]. Available: https://www.greattransition.org/archives/papers/How_Technology_Could_Contribute_to_a Sustainable_World.pdf

[86] N. Cardona-Vivas, M. A. Correa, and H. A. Colorado, "Multifunctional composites obtained from the combination of a conductive polymer with different contents of primary battery waste powders," *Sustainable Materials and Technologies*, vol. 28, Jul. 2021, doi: 10.1016/j.susmat.2021.e00281.

[87] C. F. Revelo, M. Correa, C. Aguilar, and H. A. Colorado, "Composite materials made of waste tires and polyurethane resin: A case study of flexible tiles successfully applied in industry," *Case Studies in Construction Materials*, vol. 15, Dec. 2021, doi: 10.1016/j.cscm.2021.e00681.

[88] H. A. Colorado, D. E. Mendoza, H.-T. Lin, and E. Gutierrez-Velasquez, "Additive manufacturing against the Covid-19 pandemic: a technological model for the adaptability and networking," *Journal of Materials Research and Technology*, vol. 16, pp. 1150–1164, Jan. 2022, doi: 10.1016/j.jmrt.2021.12.044.

[89] R. García-Contreras, A. Agudelo, A. Gómez, P. Fernández-Yáñez, O. Armas, and Á. Ramos, "Thermoelectric Energy Recovery in a Light-Duty Diesel Vehicle under Real-World Driving Conditions at Different Altitudes with Diesel, Biodiesel and GTL Fuels," *Energies (Basel)*, vol. 12, no. 6, p. 1105, Mar. 2019, doi: 10.3390/en12061105.

[90] B. Cai, H. Hu, H.-L. Zhuang, and J.-F. Li, "Promising materials for thermoelectric applications," *J Alloys Compd*, vol. 806, pp. 471–486, 2019, doi: 10.1016/j.jallcom.2019.07.147.

[91] H. J. Goldsmid, *Introduction to Thermoelectricity*. 2016. doi: 10.1533/9781845690915.3.339.

[92] C. Gayner and K. K. Kar, "Recent advances in thermoelectric materials," *Progress in Materials Science*, vol. 83. Elsevier Ltd, pp. 330–382, Oct. 01, 2016. doi: 10.1016/j.pmatsci.2016.07.002.

[93] B. Cai, H. Hu, H. L. Zhuang, and J. F. Li, "Promising materials for thermoelectric applications," *J Alloys Compd*, vol. 806, pp. 471–486, Oct. 2019, doi: 10.1016/j.jallcom.2019.07.147.

[94] C. N. Kim, "Development of a numerical method for the performance analysis of thermoelectric generators with thermal and electric contact resistance," *Appl Therm Eng*, vol. 130, pp. 408–417, Feb. 2018, doi: 10.1016/j.applthermaleng.2017.10.158.

[95] A. S. Korotkov, V. v. Loboda, S. B. Makarov, and A. Feldhoff, "Modeling thermoelectric generators using the ANSYS software platform: Methodology, practical applications, and prospects," *Russian Microelectronics*, vol. 46, no. 2, pp. 131–138, Mar. 2017, doi: 10.1134/S1063739717020056.

[96] S. LeBlanc, "Thermoelectric generators: Linking material properties and systems engineering for waste heat recovery applications," *Sustainable Materials and Technologies*, vol. 1–2, pp. 26–35, Dec. 2014, doi: 10.1016/j.susmat.2014.11.002.

[97] Y. M. Seo, M. Y. Ha, S. H. Park, G. H. Lee, Y. S. Kim, and Y. G. Park, "A numerical study on the performance of the thermoelectric module with different heat sink shapes," *Appl Therm Eng*, vol. 128, pp. 1082–1094, Jan. 2018, doi: 10.1016/j.applthermaleng.2017.09.097.

[98] S. Twaha, J. Zhu, Y. Yan, and B. Li, "A comprehensive review of thermoelectric technology: Materials, applications, modelling and performance improvement," *Renewable and Sustainable Energy Reviews*, vol. 65, pp. 698–726, Nov. 2016, doi: 10.1016/j.rser.2016.07.034.

[99] P. Wang, B. L. Wang, and J. E. Li, "Temperature and performance modeling of thermoelectric generators," *Int J Heat Mass Transf*, vol. 143, p. 118509, Nov. 2019, doi: 10.1016/j.ijheatmasstransfer.2019.118509.

[100] M. Zakeri, M. Allahkarami, G. Kavei, A. Khanmohammadian, and M. R. Rahimipour, "Synthesis of nanocrystalline Bi2Te3 via mechanical alloying," *J Mater Process Technol*, vol. 209, no. 1, pp. 96–101, Jan. 2009, doi: 10.1016/j.jmatprotec.2008.01.027.

[101] I. Zardo and R. Rurali, "Manipulating phonons at the nanoscale: Impurities and boundaries," *Curr Opin Green Sustain Chem*, vol. 17, pp. 1–7, Jun. 2019, doi: 10.1016/j.cogsc.2018.12.006.

[102] S. Zhuiykov, "Composite Graphene/Semiconductor Nano-Structures for Energy Storage," in *Nanostructured Semiconductors*, Elsevier, 2018, pp. 295–352. doi: 10.1016/B978-0-08-101919-1.00006-4.

[103] C. Gayner and Y. Amouyal, "Energy Filtering of Charge Carriers: Current Trends, Challenges, and Prospects for Thermoelectric Materials," *Adv Funct Mater*, p. 1901789, May 2019, doi: 10.1002/adfm.201901789.

[104] T. Hori and J. Shiomi, "Tuning phonon transport spectrum for better thermoelectric materials," *Sci Technol Adv Mater*, vol. 20, no. 1, pp. 10–25, Dec. 2019, doi: 10.1080/14686996.2018.1548884.

[105] Y. Takagiwa and Y. Shinohara, "A practical appraisal of thermoelectric materials for use in an autonomous power supply," *Scr Mater*, vol. 172, pp. 98–104, Nov. 2019, doi: 10.1016/j.scriptamat.2019.07.022.

[106] J. He, M. G. Kanatzidis, and V. P. Dravid, "High performance bulk thermoelectrics via a panoscopic approach," *Materials Today*, vol. 16, no. 5, pp. 166–176, 2013, doi: 10.1016/j.mattod.2013.05.004.

[107] O. Martin Løvvik and K. Berland, "Predicting the thermoelectric figure-of-merit from first principles," *Mater Today Proc*, vol. 5, no. 4, pp. 10227–10234, 2018, doi: 10.1016/j.matpr.2017.12.269.

[108] X. Zhou *et al.*, "Routes for high-performance thermoelectric materials," *Materials Today*, vol. 21, no. 9, pp. 974–988, 2018, doi: 10.1016/j.mattod.2018.03.039.

[109] J. Yang, F. Wu, Z. Zhu, L. Yao, H. Song, and X. Hu, "Thermoelectrical properties of lutetium-doped Bi2Te3 bulk samples prepared from flower-like nanopowders," *J Alloys Compd*, vol. 619, pp. 401–405, Jan. 2015, doi: 10.1016/j.jallcom.2014.09.024.

[110] J. An, M.-K. Han, and S.-J. Kim, "Synthesis of heavily Cu-doped Bi2Te3 nanoparticles and their thermoelectric properties," *J Solid State Chem*, vol. 270, pp. 407–412, Feb. 2019, doi: 10.1016/j.jssc.2018.11.024.

[111] C. Li *et al.*, "Simultaneous increase in conductivity and phonon scattering in a graphene nanosheets/(Bi2Te3)0.2(Sb2Te3)0.8 thermoelectric nanocomposite," *J Alloys Compd*, vol. 661, pp. 389–395, Mar. 2016, doi: 10.1016/j.jallcom.2015.11.217.

[112] Y. Geng, S. J. Wang, and J. K. Kim, "Preparation of graphite nanoplatelets and graphene sheets," *J Colloid Interface Sci*, vol. 336, no. 2, pp. 592–598, 2009, doi: 10.1016/j.jcis.2009.04.005.

[113] D. Suh *et al.*, "Enhanced thermoelectric performance of Bi0.5Sb1.5Te3-expanded graphene composites by simultaneous modulation of electronic and thermal carrier transport," *Nano Energy*, vol. 13, pp. 67–76, Apr. 2015, doi: 10.1016/j.nanoen.2015.02.001.

[114] M. L. Lwin *et al.*, "Oxide formation mechanism and its effect on the microstructure and thermoelectric properties of p-type Bi0.5Sb1.5Te3 alloys," *Intermetallics (Barking)*, vol. 103, pp. 23–32, Dec. 2018, doi: 10.1016/j.intermet.2018.09.015.

[115] A. Casian, "Violation of the Wiedemann-Franz law in quasi-one-dimensional organic crystals," *Phys Rev B Condens Matter Mater Phys*, vol. 81, no. 15, Apr. 2010, doi: 10.1103/PhysRevB.81.155415.

[116] D. Qin, F. Pan, J. Zhou, Z. Xu, and Y. Deng, "High ZT and performance controllable thermoelectric devices based on electrically gated bismuth telluride thin films," *Nano Energy*, vol. 89, Nov. 2021, doi: 10.1016/j.nanoen.2021.106472.

[117] O. Yamashita, K. Satou, H. Odahara, and S. Tomiyoshi, "Dependence of thermal conductivity on electrical resistivity in Bismuth-Tellurides," *Journal of Physics and Chemistry of Solids*, vol. 66, no. 7, pp. 1287–1293, Jul. 2005, doi: 10.1016/j.jpcs.2005.04.011.

[118] K. H. Lee, P. Dharmaiah, and S. J. Hong, "Formation mechanism of twin structures in p-type (Bi0.25Sb0.75)2Te3 thermoelectric compound," *Scr Mater*, vol. 162, pp. 437–441, Mar. 2019, doi: 10.1016/j.scriptamat.2018.12.006.

[119] S. Grasso *et al.*, "Ultra low thermal conductivity of disordered layered p-type bismuth telluride," *J Mater Chem C Mater*, vol. 1, no. 12, pp. 2362–2367, Mar. 2013, doi: 10.1039/c3tc30152d.

[120] Q. Zhang *et al.*, "Suppression of grain growth by additive in nanostructured p-type bismuth antimony tellurides," *Nano Energy*, vol. 1, no. 1, pp. 183–189, Jan. 2012, doi: 10.1016/j.nanoen.2011.10.006.

[121] N. K. Singh, J. Pandey, S. Acharya, and A. Soni, "Charge carriers modulation and thermoelectric performance of intrinsically p-type Bi2Te3 by Ge doping," *J Alloys Compd*, vol. 746, pp. 350–355, 2018, doi: 10.1016/j.jallcom.2018.02.310.

[122] T. S. Kim and B. S. Chun, "Microstructure and thermoelectric properties of n- and p-type Bi2Te3 alloys by rapid solidification processes," *J Alloys Compd*, vol. 437, no. 1–2, pp. 225–230, Jun. 2007, doi: 10.1016/j.jallcom.2006.07.090.

[123] Y. Horio and A. Inoue, “Effect of oxygen content on thermoelectric properties of n-type (Bi,Sb) 2(Te,Se) 3 alloys prepared by rapid solidification and hot-pressing techniques,” in *Materials Transactions*, May 2006, vol. 47, no. 5, pp. 1412–1416. doi: 10.2320/matertrans.47.1412.

[124] T. S. Kim and B. S. Chun, “Microstructure and thermoelectric properties of n- and p-type Bi2Te3 alloys by rapid solidification processes,” *J Alloys Compd*, vol. 437, no. 1–2, pp. 225–230, Jun. 2007, doi: 10.1016/j.jallcom.2006.07.090.

[125] A. Loaiza and H. A. Colorado, “Marshall stability and flow tests for asphalt concrete containing electric arc furnace dust waste with high ZnO contents from the steel making process,” *Constr Build Mater*, vol. 166, pp. 769–778, Mar. 2018, doi: 10.1016/j.conbuildmat.2018.02.012.

[126] H. A. Colorado, A. Muñoz, and S. N. Monteiro, “Circular Economy of Construction and Demolition Waste: A Case Study of Colombia,” *Sustainability (Switzerland)*, vol. 14, no. 12, Jun. 2022, doi: 10.3390/su14127225.

[127] H. A. Colorado and G. I. Echeverri-Lopera, “The solid waste in Colombia analyzed via gross domestic product: Towards a sustainable economy,” *Revista Facultad de Ingenieria*, no. 96, pp. 51–63, 2020, doi: 10.17533/udea.redin.20191046.

[128] J. E. Jiménez, C. M. Fontes Vieira, and H. A. Colorado, “Composite Soil Made of Rubber Fibers from Waste Tires, Blended Sugar Cane Molasses, and Kaolin Clay,” *Sustainability*, vol. 14, no. 4, p. 2239, Feb. 2022, doi: 10.3390/su14042239.

[129] G. Agudelo, C. A. Palacio, S. Neves Monteiro, and H. A. Colorado, “Foundry Sand Waste and Residual Aggregate Evaluated as Pozzolans for Concrete,” *Sustainability*, vol. 14, no. 15, p. 9055, Jul. 2022, doi: 10.3390/su14159055.

[130] W. Punin, S. Maneewan, and C. Punlek, “Heat transfer characteristics of a thermoelectric power generator system for low-grade waste heat recovery from the sugar industry,” *Heat and Mass Transfer*, vol. 55, no. 4, pp. 979–991, Apr. 2019, doi: 10.1007/s00231-018-2481-5.